Biosensors and Carbon Nanomaterials

DOI: 10.1002/anie.200903463

Carbon Nanomaterials in Biosensors: Should You Use Nanotubes or Graphene?

*Wenrong Yang, Kyle R. Ratinac, Simon P. Ringer, Pall Thordarson, J. Justin Gooding, and Filip Braet**

Keywords:
biosensors · carbon nanomaterials · carbon nanotubes · graphene · sensors

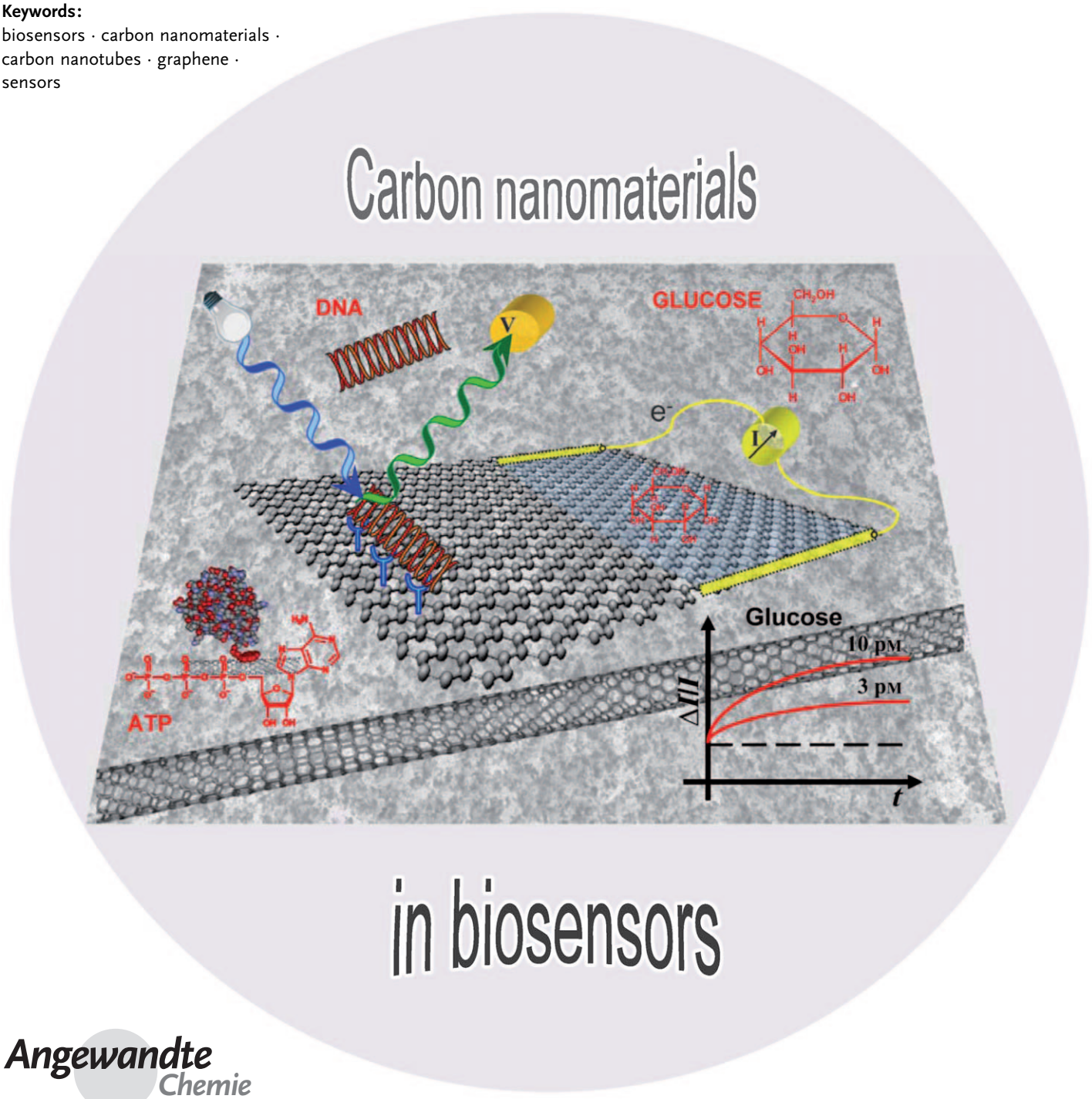

From diagnosis of life-threatening diseases to detection of biological agents in warfare or terrorist attacks, biosensors are becoming a critical part of modern life. Many recent biosensors have incorporated carbon nanotubes as sensing elements, while a growing body of work has begun to do the same with the emergent nanomaterial graphene, which is effectively an unrolled nanotube. With this widespread use of carbon nanomaterials in biosensors, it is timely to assess how this trend is contributing to the science and applications of biosensors. This Review explores these issues by presenting the latest advances in electrochemical, electrical, and optical biosensors that use carbon nanotubes and graphene, and critically compares the performance of the two carbon allotropes in this application. Ultimately, carbon nanomaterials, although still to meet key challenges in fabrication and handling, have a bright future as biosensors.

From the Contents

1. Introduction

There has been an explosion of interest in the use of nanomaterials for the development of biosensors, and carbon nanotubes (CNTs) are at the forefront of this explosion.[1–3] The interest is partly motivated by the ability to improve macroscale biosensors by incorporating CNTs, and partly by a desire to develop completely new nanoscale biosensors. However, the interest that has surrounded CNTs in general, and their use in biosensing in particular, looks like it will be dwarfed by the swell of interest in graphene. Yet obvious questions arise: What specific advantages do these two carbon nanomaterials provide over macroscopic materials in biosensors? When comparing these two carbon allotropes, does graphene possess any significant advantages over CNTs at all? And, if so, what lessons can we learn from developments in nanotube-based biosensors to expedite developments in graphene-based biosensors? Attempts to answer these three questions are the subject of this Review.

The IUPAC definition of an electrochemical biosensor states that a biosensor is a self-contained integrated device that is capable of providing specific quantitative or semiquantitative analytical information by using a biological recognition element (biochemical receptor) in direct spatial contact with a transduction element.[4] Importantly, a biosensor should be distinguished from a bioanalytical system, which requires additional processing steps, such as reagent addition. This definition places no size constraint on a biosensor, which can therefore be macroscopic, as seen in commercial glucose biosensors; can have a microscale or nanoscale sensing element packaged within a macroscopic device, as seen in field-effect transistor (FET) type devices;[5,6] or the entire device can be on the nanoscale, as demonstrated in some nanoparticle-based sensing systems.[7,8]

Nanomaterials, particularly carbon nanomaterials, have a significant role to play in new developments in each of the biosensor size domains. This significance arises as nanomaterials can help address some of the key issues in the development of all biosensors. Such issues include: design of the biosensing interface so that the analyte selectively interacts with the biosensing surface;[9,10] achievement of efficient transduction of the biorecognition event;[11,12] increases in the sensitivity and selectivity of the biosensor;[13,14] and improvement of response times in very sensitive systems.[15] More specific challenges include: making biosensors compatible with biological matrices, so that they can be used in complex biological samples or even in vivo;[16,17] fabrication of viable biosensors that can operate within confined environments such as inside cells;[17] and multiplexing biosensors so multiple analytes can be detected on one device.[18–20] Various kinds of zero-, one-, two-, and three-dimensional nanomaterials are helping to meet these challenges. Examples of such materials include semiconductor quantum dots,[21] metallic nanoparticles,[22] metallic or semiconductor nanowires,[14,23] CNTs,[24,25] nanostructured conductive polymers or nanocomposites thereof,[26] mesoporous materials,[27] and various other nanomaterials.[28,29] In this Review, however, we will focus only on the use of CNTs and graphene in biosensors.

CNTs have high aspect ratios, high mechanical strength, high surface areas, excellent chemical and thermal stability, and rich electronic and optical properties.[30] The latter properties make CNTs important transducer materials in biosensors: high conductivity along their length means they are excellent nanoscale electrode materials[31–33] (Figure 1); their semiconducting behavior makes them ideal for nano-

[*] Dr. W. Yang,[+] Dr. K. R. Ratinac,[+] Prof. S. P. Ringer, Prof. F. Braet
Australian Key Centre for Microscopy & Microanalysis
The University of Sydney
Madsen Building (F09), NSW, Sydney 2006 (Australia)
Fax: (+61) 2-9351-7682
E-mail: f.braet@usyd.edu.au
Homepage: http://www.emu.usyd.edu.au/
Dr. P. Thordarson, Prof. J. J. Gooding
School of Chemistry, The University of New South Wales
Sydney, NSW 2052 (Australia)
[+] These authors contributed equally to this work.

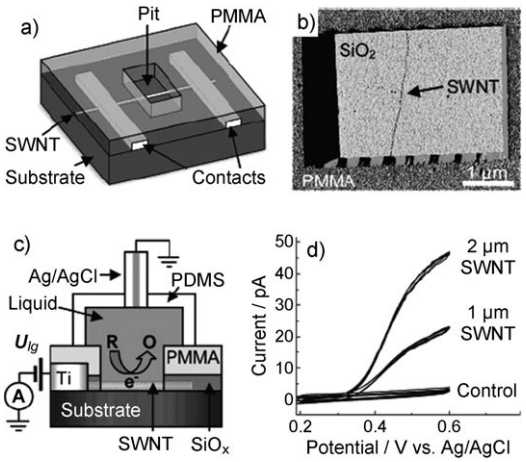

Figure 1. An example of an electrochemical sensor made from single-walled nanotubes (SWNTs): The construction (a–c) and electrochemical response (d) for a metallic-single-walled-nanotube electrode in an aqueous solution of a ferrocene derivative. (Reprinted from Ref. [31] with permission. Copyright 2006 American Chemical Society).

scale FETs,[34] and their optical properties are suitable for entirely nanoscale devices.[35,36] This combination of properties has resulted in CNTs being used to address all of the biosensing issues listed above. For example, the combination of excellent conductivity, good electrochemical properties, and nanometer dimensions has seen CNTs being plugged directly into individual redox enzymes for better transduction in electrochemical enzyme biosensors.[37–41] Moreover, alignment of CNTs has created the potential for electrodes that resist nonspecific adsorption of proteins, but that can interface to individual biomolecules.[42–44] FET biosensors based on CNTs[44,45] hold the promise of detecting single-molecule events.[46] The sensitivity of the optical properties of CNTs to binding events has also been exploited to make entirely nanoscale, but highly sensitive, multiplexed optical biosensors that could be used inside cells or dispersed through a system to capture the small amount of analyte in a sample.[47]

The success of CNTs in advancing biosensors is part of the reason for the incredible interest in graphene as a material that could potentially push the boundaries of this field even farther. Yet CNTs are commonly referred to as rolled up graphene sheets, and both allotropes have a meshwork of sp^2-hybridized carbon atoms, so the question arises as to whether graphene offers any real benefits in properties relative to CNTs. Given the identical composition of nanotubes and graphene, one could be forgiven for suspecting that their properties would also be similar; however, this is not always the case, as we shall see shortly, and the differences in structure and properties open new vistas for further developments in biosensors.

In this Review, we aim to discuss the recent advances in biosensors made with CNTs and graphene. Firstly, we will briefly discuss the relevant properties of these two materials in the context of biosensors. The application of CNTs in biosensors will then be discussed, with a focus on some of the more significant conceptual advances that have been made, rather than trying to comprehensively cover all the work performed in this vibrant field—a task that would be almost impossible. This section will start with electrochemical biosensors, which typically are macroscale biosensors fabricated with nanomaterials; it will then move onto FET-based devices where, in many cases, the transducing element is nanoscale; and it will conclude with the limited work on using CNTs in nanoscale optical biosensors. The section on graphene will attempt to be comprehensive, as papers in this area are just beginning to emerge. It will briefly explain methods of producing graphene and then explore sensing devices that have been made with graphene as the transducing element. The Review will be completed by seeking to answer the three questions raised above, and by discussing some of the challenges in continued development of biosensors that incorporate CNTs or graphene.

2. Uncommon Carbon: An Introduction to CNTs and Graphene

Any biosensor based on CNTs or graphene should ideally be designed to exploit the unique properties of each nanomaterial. With this in mind, therefore, we will provide a brief introduction to the rather special structures and properties of these two allotropes of carbon (Figure 2).

2.1. Basic Structure and Properties of CNTs

CNTs are well-ordered, hollow graphitic nanomaterials made of cylinders of sp^2-hybridized carbon atoms. These materials are classed as single-walled nanotubes (SWNTs), which are single sheets of graphene "rolled" into tubes, or

Wenrong Yang was born in China, and received his PhD degree in chemistry in 2002 from the University of New South Wales under the mentorship of Prof. Justin Gooding and Prof. Brynn Hibbert. He currently a is University of Sydney Research Fellow, working on biological and biomedical applications of CNTs and graphene with A/Prof. Filip Braet. He also is exploring single-molecule conductivity by scanning probe microscopy.

Since completing his PhD in ceramic engineering, Kyle Ratinac has carried out research on various nanomaterials, including polymer nanocomposites and nanoparticles. He is Research Development Manager of the Australian Key Centre for Microscopy and Microanalysis at the University of Sydney.

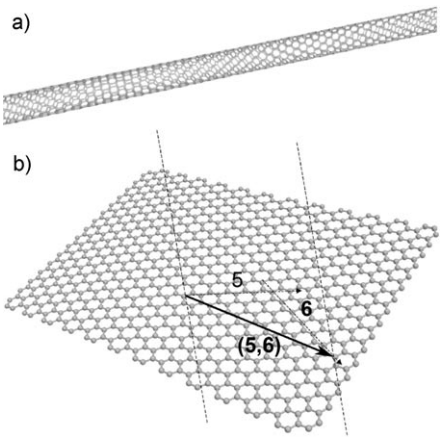

Figure 2. The ideal structures of a) a single-walled nanotube and b) a graphene sheet. As an example, the chiral vectors required to roll up a (5,6) nanotube from a piece of the graphene are also illustrated (see Section 2.1).

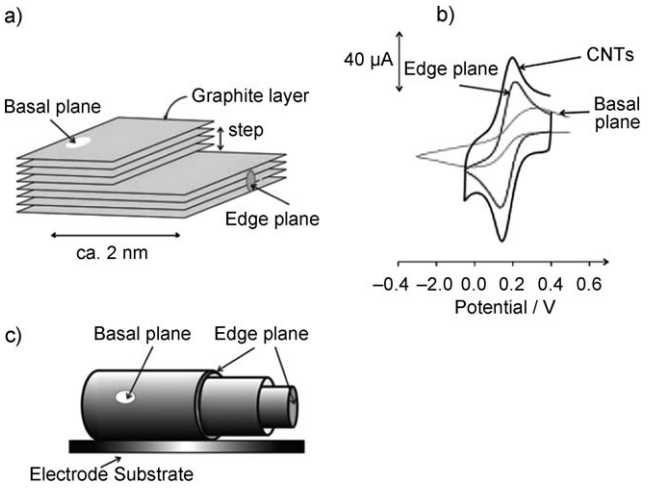

Figure 3. a) Representation of a crystal of highly ordered pyrolytic graphite (HOPG) in which the layers of graphite have an interlayer spacing of 3.35 Å. b) The difference in the voltammetric response for the reduction of hexacyanoferrate ions in an aqueous solution by using basal-plane or edge-plane HOPG electrodes or CNT-based electrodes. Note the identical response for the CNT-modified electrode and the edge-plane HOPG electrode. c) A single MWNT on an electrode surface where the edge-plane-like sites are shown at the end of the tube and the basal-plane-like sites lie along the tube axis. Reprinted from Ref. [56].

multiwalled nanotubes (MWNTs), each of which contains several concentric tubes that share a common longitudinal axis.[30,48] As one-dimensional carbon allotropes, CNTs have lengths that can vary from several hundred nanometers to several millimeters, but their diameters depend on their class: SWNTs are 0.4–2 nm in diameter and MWNTs are 2–100 nm in diameter. In addition, MWNTs can occur in various morphologies such as "hollow tube", "bamboo", and "herringbone", depending on their mode of preparation.[49–52] The electronic properties of SWNTs are controlled by the chirality, that is, the angle at which the graphene sheets roll up and hence the alignment of the π orbitals.[53,54] This angle can be quantified by the chirality vector (n,m), where n and m are the (integer) numbers of hexagons traversed in the two unit-vector directions, $\mathbf{a_1}$ and $\mathbf{a_2}$, of the graphene lattice such that, when rolled up to touch the tip of the vector to its tail, the graphene would form the desired nanotube (Figure 2b). This vector can be directly related to electronic properties in so far as the resulting SWNT will be metallic if $(n-m)$ is a multiple of 3; otherwise, it will be a semiconductor.[55]

An important aspect of the structure of CNTs is their local anisotropy, which arises because the walls of the tubes are very different from their ends. The sidewalls are a relatively inert layer of sp^2-hybridized carbon atoms, somewhat analogous to the basal planes of pyrolytic graphite; the open ends or "tips" of nanotubes have carbon atoms bonded to oxygen to give far more reactive species, much like the edge planes of pyrolytic graphite (Figure 3).[56] This structural heterogeneity has hindered our understanding of the electrochemistry of CNTs because, when incorporated into electrodes, the rate of electron transfer depends critically on the nanostructure of the electrode surface and particularly on the nanotube orientation and arrangement, factors that frequently are not quantified.[57] Additional uncertainty arises over whether the electrochemistry of CNTs is determined by their inherent properties, by variable levels of oxygen-containing groups or edge defects on the tips, or by remnant catalytic particles that remain in the tubes even after purification.[58–61] There is evidence, for example, that the favorable electrochemical properties of SWNT-modified electrodes arise from oxygenated carbon species, especially carboxyl moieties, which are produced on the tips of the nanotubes during acid purification.[40,50,62] Conversely, other work has found that increased concentrations of oxygen-containing groups on double-walled or multiwalled CNTs[63,64] and graphite[65] actually slow the rate of heterogeneous electron transfer. In fact, Pumera et al.[66] consider that oxygen-containing groups play a minor role in heterogeneous electron transfer for electrochemically activated MWNTs, and suggest instead that the increased heterogeneous electron-transfer rate lies in an increase of the density of edge-like sites on the sidewalls of the tubes. In an effort to overcome some of this uncertainty, Dai and co-workers recently carried out an elegant experiment with superlong (5 mm), vertically aligned CNTs (Figure 4).[67] By selectively masking the sidewalls or tips with a nonconducting polymer coating and by controlling the level of oxidation, they were able to explore the relative contributions of sidewalls, tips, and oxidation state in CNT electrochemistry. It turned out that the relative importance of these factors varied with the type of redox probe investigated and the redox reaction involved. For example, the faradaic electrochemistry of potassium hexacyanoferrate ($K_3[Fe(CN)_6]$) was much enhanced at the CNT tips, especially in the presence of oxygen-containing moieties, whereas the electron-transfer kinetics were slower and less pronounced at the sidewalls. In contrast, the oxidation of hydrogen peroxide (H_2O_2) occurred more readily at sidewalls than at tips, but was relatively insensitive to the presence of oxygen-containing groups. The redox reactions of nicotinamide adenine dinucleotide dehydrogenase (NADH) and ascorbic acid displayed different trends again.

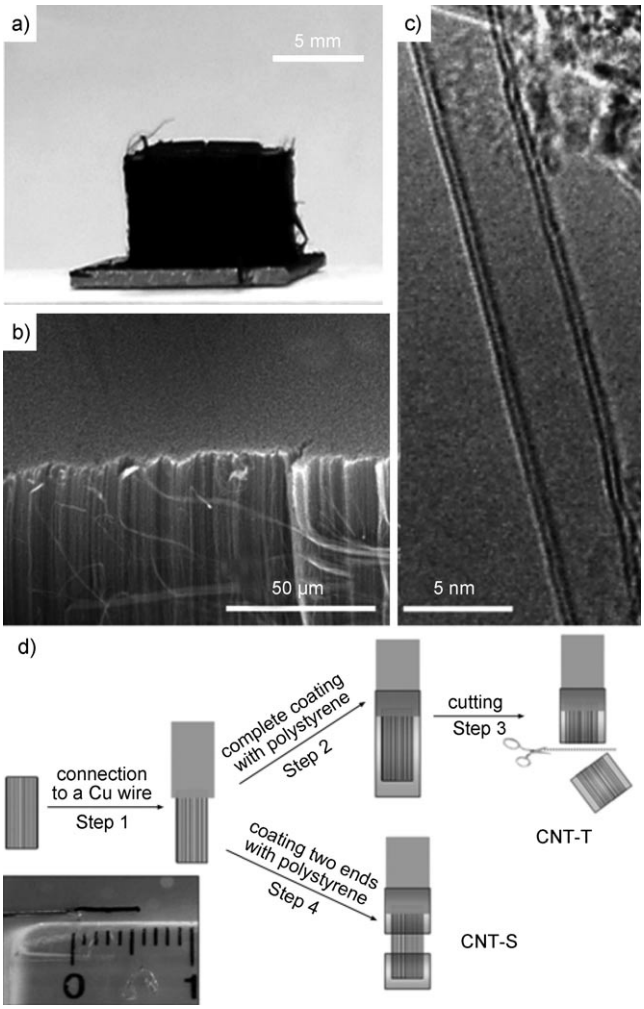

Figure 4. a) Digital photograph, b) SEM image, and c) TEM image of the aligned superlong CNTs, as synthesized. d) A schematic representation of the procedure for preparing the CNT electrodes with only the nanotube tip (CNT-T) or sidewall (CNT-S) accessible to electrolyte. The inset in (d) shows a digital photograph of a nanotube electrode prepared with an aligned superlong CNT bundle connected to a copper wire. Reprinted from Ref. [67].

The other major source of conflict in reports of electrochemical behavior of CNTs is compositional heterogeneity. In theory, CNTs are pure carbon; in reality, they almost always contain some impurities, such as 1) metallic compounds or nanoparticles derived from the catalysts used in nanotube growth, which can remain trapped between the graphene sheets in nanotubes even after extensive acid washing,[58,61] and 2) oxygen-containing moieties created during the washing steps. These impurities, particularly the metallic compounds, are probably responsible for the "electrocatalysis" seen at some nanotube-modified electrodes.[56] Careful work on the removal of these metallic nanoparticle impurities, however, suggests that, despite the plethora of reports stating that carbon nanotubes have better electrochemical properties than other electrode surfaces, the electrochemical properties of CNTs might be no better than edge planes of highly ordered pyrolytic graphite (HOPG).[68,69] However, HOPG cannot be engineered to such small sizes as CNTs. The very recent discovery of methods for producing SWNTs without the use of iron-group catalysts[70,71] offers metal-free CNTs whose properties are not obscured by the catalyst impurities. This advance will provide a route to a clearer understanding of which electrochemical properties are intrinsic to nanotubes and which properties are not.

Our knowledge of the electronic properties of CNTs is quite mature compared with our understanding of their electrochemistry. MWNTs are metallic conductors, whereas SWNTs can be metallic or semiconductors, depending on their diameter and chirality. For small-diameter SWNTs, approximately two-thirds are semiconductors and one-third is metallic.[30,72] For semiconducting nanotubes, the band gap also depends on tube diameter. Consequently, to achieve uniform electrical (and optical) properties, SWNTs have to be monodisperse in diameter and in chirality, because SWNTs with almost identical diameters can have different chiral vectors and hence different electronic properties. Even then, SWNTs with identical chiral vectors can possess different chiral handedness, which will influence the interaction of SWNTs with circularly polarized light. Therefore, much research effort in recent years has been seeking large-scale, economical production of monodisperse SWNTs, with control of electronic type, diameter, length, and chiral handedness.[48,73] However, of the many techniques developed, none has overcome all the obstacles to date.

Like their electronic properties, the dominant optical transitions in SWNTs depend on their diameters and chiral vectors. Thus, the heterogeneity of band structures, lengths, and defects produced in most samples of nanotubes means that spectral measurements give ensemble-average properties only. Despite this limitation, the optical properties of SWNTs have attracted growing interest since the observation of near-infrared (NIR) luminescence from well-separated, surfactant-suspended semiconducting SWNTs in 2002.[74] Subsequent photoluminescence excitation measurements resulted in the precise mapping of the transition energies for a large variety of specific semiconducting structural species.[75] Measurements on single tubes have helped eliminate the inhomogeneity present in the optical spectra of bulk SWNTs.[76] For instance, photoluminescence studies, though limited to semiconducting SWNTs, have revealed the true line width of emission spectra and the presence of spectral variations.[77] Raman scattering has also been used to study individual semiconducting and metallic SWNTs,[78] but such experiments are constrained by the weak signal and the need to use near-resonant laser sources. Highly sensitive imaging and absorption spectroscopy of individual tubes is possible through photothermal heterodyne imaging.[79] A particularly exciting development is monitoring single-molecule chemical reactions with individual SWNTs by NIR photoluminescence microscopy, in which the emission intensity within distinct sub-micrometer segments of single tubes changes in discrete steps as reactions occur with single acid, base, or diazonium molecules.[80] These developments have laid the mechanistic groundwork for SWNTs to function as single-molecule stochastic biosensors.[47,81]

2.2. Basic Structure and Properties of Graphene

The idealized structure of graphene is completely two-dimensional. It comprises a single layer of sp^2-hybridized carbon atoms joined by covalent bonds to form a flat hexagonal lattice.[82] Practically, however, the structure is complicated by the difficulty in isolating single layers of graphene in a controlled manner. Often, this means that what is termed "graphene" actually comprises stacks of graphene layers, each containing different numbers of atomic sheets. Therefore, it is essential to measure the number of layers by, for example, atomic force microscopy,[83] Raman spectroscopy,[84] contrast spectroscopy,[85] or low-energy electron microscopy (LEEM)[86] to determine if one is dealing with single-layer graphene, a bilayer, few-layer graphene (3–9 layers[87]), or even multilayer graphene (or "thin graphite").[83,88] The other complicating factor in graphene's structure is that it is never atomically flat because of its flexibility, which means that the sheets tend to curl, fold, and corrugate (Figure 5). The large folds and pleats tend to arise from processing issues,[83,89] whereas smaller ripples tend to be inherent in the structure of its isolated layers.[90–93]

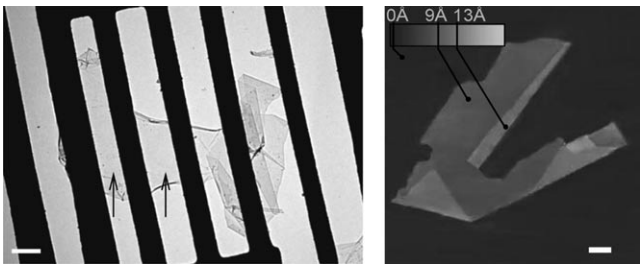

Figure 5. Left: Bright-field TEM image of a graphene membrane suspended across metal bars. Its central part (the homogeneous and featureless region indicated by arrows) is single-layer graphene. Electron diffraction images from different areas of the graphene flake (not shown) demonstrate that it is a single crystal without domains. Note the scrolled top and bottom edges and the folded region on the right. Scale bar: 500 nm. (Reprinted by permission from Macmillan Publishers Ltd: Nature [90], copyright 2007.) Right: Flakes of graphene on top of an oxidized Si wafer as visualized by AFM; once again, folds are evident. Scale bar, 1 μm. (Reprinted from Ref. [89].)

Unsurprisingly, this essentially two-dimensional form of carbon displays many unique properties. We will provide only a short survey of graphene's electrochemical, electronic, and optical properties because these are most relevant to biosensor applications. For more detailed presentations of such properties, see recent reviews.[82,87,94–96]

Despite the uncertainties that remain about the electrochemistry of CNTs, the electrochemistry of graphene is even less clear. This is primarily because there have been so few studies of electrochemical properties, and those that are available were performed with varying forms of "graphene",[97–105] thus making it difficult to draw general conclusions. Still, there is evidence that graphene and its derivatives can exhibit good electrochemical performance compared with other electrodes such as glassy carbon,[99] graphite,[104] or even CNTs.[100,105] Thus far, however, the graphene-modified electrodes have not been compared with the most appropriate control electrodes of basal- and edge-plane HOPG, and seldom has the graphene material been characterised in detail. These issues also limited many of the early studies on CNT-modified electrodes. Nevertheless, multilayer graphene has been found to display single-electron Nernstian behavior, with rapid electron transfer, when used as an electrode in cyclic voltammetry of $[Fe(CN)_6]^{3-/4-}$ solutions.[99] This kind of electrode also showed favorable electrochemical properties, thus allowing a clear separation of redox peaks in mixtures of biological molecules that only appeared as a single broad peak at higher potentials for glassy carbon electrodes. Similarly, excellent electrochemistry has been observed for redox reactions of biomolecules[100,105] or drugs[102] when electrodes have incorporated graphene oxide or reduced graphene oxide. The origin of these intriguing properties remains an open question, although the edges seem likely to be the primary sites of electrochemical reactions in graphene, while the functional groups and defects probably are also important in (reduced) graphene oxide.

The first properties of graphene to be studied were its electronic properties,[83] which have thus been the focus of the majority of research to date. The electronic properties originate largely in the delocalized π bonds above and below the basal plane, which arise from the sp^2 hybridization responsible for graphene's layered structure. These delocalized electrons, and the quality of the graphene lattice, create high electrical conductivities and mobilities: room-temperature mobilities in graphene with one to three layers have been measured at 15000 $cm^2 V^{-1} s^{-1}$ or more,[83,106] while clean, suspended single layers achieved 230000 $cm^2 V^{-1} s^{-1}$ at temperatures near absolute zero.[107] Graphene also shows an ambipolar electric-field effect in which negative gate voltages induce large concentrations of holes, while positive voltages induce large numbers of electrons. This behavior appears as a spike in resistivity at zero gate voltage in pristine graphene.[83,106] Other electronic properties tend to be highly sensitive to the number of layers in the stack, because this variable causes sizeable changes in band structure and band overlap. A single layer, for example, is a zero-gap semiconductor. While this is also true of a bilayer, in this case a band gap is developed during the application of a gate voltage.[108] A trilayer, which is a semimetal, shows a gate-voltage-tunable band overlap,[109] and the extent of overlap between the conduction and valence bands increases as additional numbers of layers are added until behavior approximating that of graphite is attained at some 12–15 layers in total.[110,111] The properties of the charge carriers in graphene, which also vary with the number of layers, are quite remarkable too, with low masses (actually attaining zero mass in a single layer) and Fermi velocities on the order of 10^6 ms^{-1}.[106,112–114] More details can be found in recent reviews.[82,87,94]

The optical properties of graphene have received considerable attention, especially as Raman and infrared spectroscopy can provide detailed information about its band structures.[112,113,115–119] Raman spectra also allow identification of the number of layers in graphene stacks because of the changes in band shape with layer number.[120] Overall, there

are two highly characteristic Raman bands in graphene: the G band at approximately 1580 cm^{-1} and the D′ band (or 2D or D* band; equivalent to the G′ band in graphite) at about 2700 cm^{-1}.[84,95,120–122] A further D band at approximately 1350 cm^{-1} occurs at the edges of sheets or in defective graphene.[120,121] For a detailed description of the Raman spectra of graphene, see the recent review by Malard et al.[95] Another interesting optical property of graphene is that, for the first four or five layers, it shows virtually constant and additive absorbance in the visible-light region. For each layer, the absorbance, which is equal to the fine-structure constant multiplied by π, is approximately 2.3 %.[123]

Table 1 summarizes some of the key factors that influence graphene's electrical and optical properties. Clearly these factors will need to be considered, and controlled where possible, during fabrication of graphene-based biosensors.

3. Recent Developments in the Use of CNTs in Biosensors

A key goal of modern science is to monitor biomolecular interactions with high sensitivity in real time, with the ultimate aim of detecting single-molecule processes in natural samples.[137–139] Today, a number of practical biomolecule-detection methods exist that can sense molecules such as DNA and proteins, but few methods have attained this ultimate goal. The unusual properties of CNTs, such as their small size and high conductivity, are allowing development of new types of electrochemical, FET-based and optical biosensors that, as we will show in the following section, are beginning to put single-molecule and single-cell detection within reach.

Table 1: Major factors that influence graphene's properties, and examples to illustrate their effects.

Factor	Effects
Number of layers	This is a primary determinant of properties. Increasing the number of layers increases the complexity of the electronic band structures, thereby changing the electrical and optical properties. For example: · Moving from single layers to trilayers changes the effective masses and the mobilities of charge carriers, the anomalous quantum Hall effects and the band gaps.[106,108,109,124] · The position and shape (i.e., component bands) of Raman spectra change with layer number.[119,120]
Substrate	The substrate's close contact with the two-dimensional graphene layer(s) has a pronounced effect: · SiO_2 substrates limit carrier mobility by more than an order of magnitude, primarily because of charged impurities in the substrate and remote interfacial phonon scattering.[125] · Suspending single-layer graphene reduces substrate effects to achieve mobilities of at least 60000 $cm^2V^{-1}s^{-1}$ and as high as 230000 $cm^2V^{-1}s^{-1}$ under vacuum at 5 K.[107] · Epitaxial few-layer graphene undergoes a binding-energy shift of the 1 s level because of charge transfer from the SiC substrate.[126] · Misfit-induced compressive strains in epitaxial graphene on SiC cause sizable blue shifts in graphene's Raman bands.[127]
Adsorbed impurities	Adsorbed gaseous species or processing impurities are hard to avoid and, with graphene's large surface area, can have substantial effects: · Adsorbed water vapor dopes graphene FETs, shifting the neutrality point (peak resistivity) to a gate voltage of about 40 V.[83] The presence of oxide capping layers or lithography residues also shifts this point.[128] · Large (ca. 3–10 times) increases in mobilities occur for suspended single-layer graphene when "current annealed" to approx. 600 °C to desorb hydrocarbon impurities.[107]
Flatness	The inherent rippling in graphene influences its properties: · Rippling causes electron and hole "puddles",[129] particularly at low concentrations of induced charge carriers.[87] · Shifts in Raman peaks occur for parts of graphene that are supported across, but not touching, the substrate.[92]
Defects	Defects in the normally high-quality graphene lattice have large effects on electronic properties and chemical affinities: · High-temperature oxidation introduces defects in the layers (shown by the weak D band in Raman spectra), thus substantially reducing the carrier mobility.[128] · Creation of graphene oxide substantially increases the hydrophilicity of graphene layers, but reduces conductivity by many orders of magnitude.[130,131] · Stacking disorder causes changes in electronic band structures.[132]
Size of sheet	Decreasing the width of graphene nanoribbons increases electrical resistivity,[133] while decreasing the size of larger sheets increases electrical noise in graphene FETs.[134]
Edge types and functionalization	Though hard to measure, let alone control, the atomic type, amounts and functional groups on the edges of graphene also alter properties: · As reviewed by Enoki et al.,[135] the amounts and distributions of armchair and zigzag edges play a critical role in the electronic and (predicted) magnetic properties of nanoscale graphene (e.g., nanoribbons or quantum dots); likewise, the types of functionalization of the edges affect these properties. · Edge roughness changes the edge states.[82] · Different amounts of edge groups affect the amount of warping of graphene.[136]

Nevertheless, an essential point to note throughout the following discussion is that most reports of biosensing deal with proofs of concept and so use biological solutions or samples made in the laboratory, rather than natural samples of, for example, urine, blood, serum, or cerebrospinal fluid, which are much more complicated. In the rare cases where clinical or other natural samples have been used in any of the cited work, we will mention it.

3.1. Electrochemical Biosensors

Electrochemical detection offers several advantages over conventional fluorescence measurements, such as portability, higher performance with lower background, less-expensive components, and the ability to carry out measurements in turbid samples. During the past few years, there have been many reports of CNT-based electrochemical biosensors for the detection of diverse biological structures such as DNA, viruses, antigens, disease markers, and whole cells. An important part of the success of CNTs for these applications is their ability to promote electron transfer in electrochemical reactions.[50,57,140]

One of the major challenges, however, for the design of electrochemical biosensors with CNTs is how to incorporate these nanomaterials into bulk electrodes for best effect. This challenge is particularly pertinent given the anisotropy of nanotube properties outlined above. Thus it is essential to understand the three main types of nanotube-derived electrodes before we consider their recent use in electrochemical biosensors. The first, and most commonly used, electrode has nanotubes "randomly distributed" on its surface (which often means an unknown configuration rather than genuinely randomized configuration). The prevalence of this approach is primarily because it is easy to achieve, not necessarily because it offers the best performance. However, recent work to fabricate random networks of chemical-vapor-deposited SWNTs has produced electrodes that are significantly faster than conventional metal-disc-based ultra-microelectrodes.[141] The second class of electrodes use aligned nanotubes to optimize electrode performance. This geometry can be achieved by self-assembly (Figure 6)[142,143] or by growing aligned nanotubes directly from a surface;[144] in the latter approach, growth of aligned SWNT "forests" is an especially interesting development.[145–147] Electrodes made with nanotubes aligned normal to the electrode surface exhibit faster heterogeneous electron transfer compared with randomly distributed arrays.[143,148] This effect occurs because the nanotube tips typically facilitate more rapid electron transfer than sidewalls, and because the electrons are only required to travel down one tube, rather than having to jump from tube to tube, in order to be transferred to the bulk electrode.[33] The third type of electrode avoids the use of ensembles of many tubes with variable properties, and instead uses a single CNT as a nanoelectrode. This is probably the most attractive design of CNT electrode, despite the challenges of fabricating and manipulating a single-CNT probe. These types of electrodes can be made with single MWNTs[149] or single SWNTs,[150] which give different electrochemical performance.

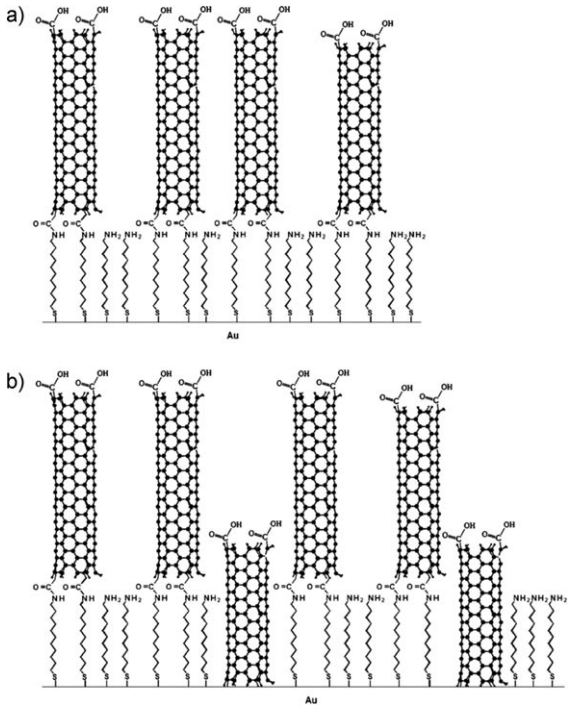

Figure 6. Illustrations of the construction of chemically aligned, oxidatively shortened nanotubes. Two possible electron-transport mechanisms are shown: a) nanotubes vertically aligned on aminoalkanthiol self-assembled monolayer (SAM), in which the electron tunnels through the nanotube and through the aliphatic chain of the alkanethiol monolayer; or b) tubes penetrating between the SAM to form a direct link with the gold, held in place by hydrophobic interactions with the SAM. (Reprinted from Ref. [143] with permission. Copyright 2009 American Chemical Society.)

When it comes to electrochemical biosensing, CNT-modified electrodes appear to offer substantially improved amperometric biosensors, with particularly enhanced sensitivity to H_2O_2 and NADH. However, as discussed above in Section 2.1, a big issue for such applications is sample purity and whether it is the nanotubes or impurities, such as residual metal catalyst particles, that provide the favorable electrochemical properties. For instance, Wang and co-workers used Nafion, a sulfonated tetrafluoroethylene-based polymer, to incorporate MWNTs into composite electrodes for glucose oxidase based detection of glucose, a process that involves the oxidation of glucose by the oxidase enzyme and then measurement of the resulting H_2O_2 concentration.[151] The composite electrodes offered substantially greater sensitivity to glucose, in particular at low potentials (−0.05 V), with negligible interference from dopamine, uric acid, or ascorbic acid, which are biological molecules that commonly interfere with electrochemical detection of glucose. It was also found that CNT-modified electrodes can accelerate electron transfer from NADH molecules, decreasing the overpotential, and minimizing surface fouling, which are properties that are particularly useful for addressing the limitations of NADH oxidation at ordinary electrodes.[152] Similar improvements in electrode performance were more recently observed for composite electrodes made with CNTs and ionic liquids, which offer high stability, high electrical conductivity, and

extremely low vapor pressure.[153,154] However, caution is needed when interpreting these results. The mechanism of favorable electrochemistry for CNT-based electrodes remains controversial because, as we discussed above, most CNTs contain metal impurities derived from the catalysts used in their growth, which are at least partially responsible for the observed electrochemical activity. Although they complicated the fundamental electrochemistry, such remnant metal nanoparticles had one benefit: they provided a clear indication that the electrochemical properties of sensors could be enhanced by deliberately integrating catalytic nanoparticles within CNTs (see below).

CNTs also offer more efficient ways of communicating between sensor electrodes and the redox-active sites of biological molecules, which are frequently embedded deep inside surrounding peptides. The high aspect ratio and small diameters of SWNTs make them suitable for penetrating through the molecule to the internal electroactive sites, while the rapid electron-transfer kinetics at the tip of oxidized tubes can enhance electron transfer. A major step in this direction was accomplished when microperoxidase-11 (MP-11)—an 11 amino acid sequence that contains a heme center and is derived from the proteolytic digestion of heme proteins—was attached to the ends of SWNTs, which were self-assembled normal to the electrode surface to produce a nanoelectrode array.[38] The high efficiency of the nanotubes as molecular wires was demonstrated by the calculated rate constant of heterogeneous electron transfer, 3.9 s^{-1}, between the electrode and the MP-11 molecules. Similarly, by using enzymes covalently attached to the ends of aligned SWNT "forest" arrays, Yu et al. reported quasi-reversible Fe^{III}/Fe^{II} voltammetry for the heme enzymes myoglobin and horseradish peroxidase.[39]

Another elegant application of CNTs to immunoassays involved forming a "forest" of SWNTs oriented perpendicularly to the basal plane of abraded pyrolytic graphite, and exploiting the high surface areas of MWNTs for delivery of the label molecules (Figure 7).[155] In this electrochemical-based sandwich immunoassay, the CNTs were used both as "nanoelectrodes", which coupled primary antibodies (Ab_1) to the pyrolytic graphite electrode, and as "vectors" in suspension that hosted multiple secondary antibodies (Ab_2) and multiple copies of the electrochemical label horseradish peroxidase (HRP). Amplified sensing signals resulted from using Ab_2-MWNT-HRP bioconjugates, which had high HRP/Ab_2 ratios, instead of conventional single-HRP labeled Ab_2. The sensing process occurred in three steps. Firstly, the Ab_1 recognized and bound the prostate specific antigen (PSA), a prostate-cancer biomarker, present in serum. Secondly, the application of Ab_2-MWNT-HRP bioconjugates targeted the now surface-tethered PSA, binding through Ab_2. Thirdly, addition of H_2O_2 allowed the indirect detection of PSA by measuring the electrochemical voltage derived from the reaction between the added H_2O_2 and the HRP on the nanotube complexes. Two points are particularly noteworthy about this approach. The first point is that the MWNTs can bind multiple HRP molecules—in contrast to Ab_2 molecules, which have only a limited labeling and binding capacity because of their size and chemistry—so that this approach could increase the detection sensitivity for PSA some 10–100 times compared to the commercial clinical immunoassays presently available. The second point is that the clinical potential of this biosensor was demonstrated by direct measurement of PSA concentration in samples of human serum from patients with cancer and from healthy subjects.

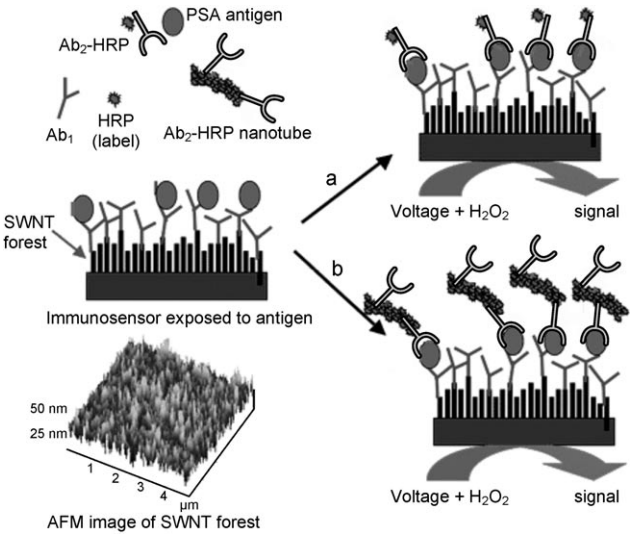

Figure 7. Construction of sensors made from primary antibodies (Ab_1), secondary antibodies (Ab_2), horseradish peroxidase (HRP), and a "forest" of SWNTs atop a pyrolytic graphite electrode. Compare the amount of label, and the size of the electrochemical signal generated, when using a) Ab2-HRP versus the b) Ab2-MWNT-HRP bioconjugates. (Modified image; reprinted from Reference [155] with permission. Copyright 2006 American Chemical Society).

The properties of CNTs can also be capitalized on by combining them with other functional materials, such as conducting polymers or metal nanoparticles, in order to enhance their electrochemical sensing performance.[52] Some examples have already been given above of the greater sensitivity obtained when CNTs are incorporated into electrodes made with polymers or ionic liquids.[151–154] Gao et al. have also reported glucose biosensors based on aligned CNTs coated with a conducting polymer.[156] The polymer was a bioactive, conducting, coaxial sheath around the individually aligned CNTs that led to low-potential detection of the H_2O_2 liberated by glucose oxidase. More recently, Dai and co-workers developed a versatile and effective approach for decorating CNTs with metallic nanoparticles;[157,158] these CNTs had enhanced electrochemical activity when incorporated into working electrodes. By also drawing on a composite system, Fisher and co-workers created a SWNT-based electrochemical biosensor that used Au-coated Pd (Au/Pd) nanocubes to enhance electrochemical activity, provide selective biofunctionalization docking points, and improve biocompatibility (Figure 8).[159] The Au/Pd nanocubes, which were of homogeneous size and shape, were integrated within an electrically contacted network of SWNTs. The Pd provided a low-resistance contact between the SWNT and Au interfaces, while the Au offered the biocompatibility necessary for biofunctionalization, potentially with a myriad of ligands and other important biomarkers. By using this unique electrode

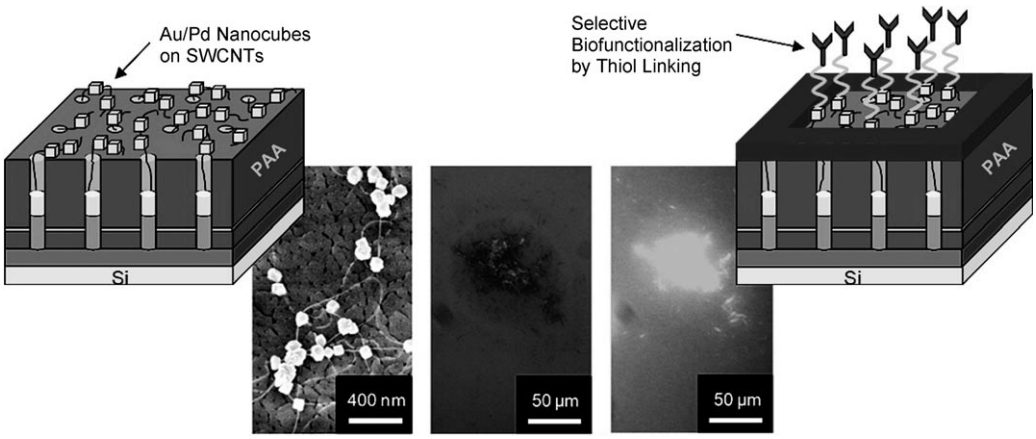

Figure 8. Networks of SWNTs decorated with Au-coated Pd (Au/Pd) nanocubes are employed as electrochemical biosensors that exhibit excellent sensitivity (2.6 $mA\,mM^{-1}\,cm^{-2}$) and a low estimated detection limit (2.3 nM) at a signal-to-noise ratio of 3 in the amperometric sensing of hydrogen peroxide. (Reprinted from reference [159] with permission. Copyright 2009 American Chemical Society.)

structure, the team showed amperometric detection of H_2O_2, thus illustrating the effectiveness of the nanocube–SWNT biosensor for glucose sensing. A clear advantage of this electrochemical decoration is that the SWNTs serve as a nucleation site for nanoparticle growth at defects in the nanotubes and as an inherent electrical contact to the nanoparticles for direct integration into devices.

An emerging trend is the move, away from just sensing molecules, towards interaction with, and sensing of, whole cells. Interactions between various cell lines and CNTs have been previously reported, and have included the adhesion, growth, and differentiation of neuronal cells on CNT-based substrates.[160] The strong interest in interfacing neuronal cells and CNTs is not accidental. The unique mechanical, chemical, and electrical properties of CNTs make them one of the most promising materials for applications in neural biosensing.[161] The high stiffness of nanotubes is important because the electrodes need to penetrate tissue, and the ability to operate as ballistic conductors—materials that do not significantly slow down the flow of electrons—should aid in lowering impedance and increasing charge transfer. Keefer and co-workers have investigated the use of nanotube-coated electrodes in preparing brain–machine interfaces, thus demonstrating that the material also appears to be biocompatible.[162] Kotov and co-workers fabricated layer-by-layer-assembled composites from SWNTs and laminin,[163] which is an essential part of human extracellular matrix. These laminin–SWNT thin films were found to encourage differentiation of neural stem cells and to be suitable for their successful excitation. Extensive formation of functional neural networks was observed, as indicated by the presence of synaptic connections. These results show that protein–SWNT composites can likely serve as materials for neural electrodes, with structures that are better adapted for long-term integration with the neural tissue. Another significant advance is the work by Lin et al., in which a sensor was devised for continuous and simultaneous monitoring of glucose and lactate in rat brain tissue.[164] The research group prepared a complex electroanalytical system in which SWNTs were loaded with glucose dehydrogenase or lactate dehydrogenase, respectively, for real-time monitoring of the metabolic intermediate glucose or the circulatory impairment molecule lactate.

In all these cases, however, more work needs to be done to assess the possible adverse immune responses that CNTs might generate in the long term, once applied in genuine clinical settings.[165] It is conceivable, for example, that CNTs might provoke the release of lymphocyte-derived cytotoxic cytokines and hence might affect the patient's overall health.[166] A partial solution to this largely unexplored problem is to make CNTs more biocompatible, which can be achieved by biochemical functionalization with biomolecules such as DNA.[1] Photochemistry[167] and wet chemistry[168] have been used to achieve efficient binding of DNA on the sidewalls and tips of CNTs. Besides reducing possible adverse effects of nanotubes, such functionalization often enhances their effectiveness in biosensors. For example, DNA-immobilized aligned CNTs have demonstrated abilities in detecting complementary DNA with a high sensitivity and selectivity.[169,170]

Another interesting development in electrochemical biosensors is the use of aptamers. These structures are oligonucleotide sequences that can be generated to have affinity for a variety of specific biomolecular targets such as drugs, proteins, and other relevant molecules. Aptamers even hold potential for use in novel therapies, and are also considered as highly suitable receptors for selective detection of a wide range of molecular targets, including bacteria.[171] Furthermore, aptamers can self-assemble on CNTs through π stacking between the nucleic acid bases and the nanotube walls. Consequently, considerable efforts have been directed towards incorporating aptamers and CNTs into the design of biosensors.[16] Very recently, Rius and co-workers reported a novel potentiometric biosensor made with aptamer-modified SWNTs that allowed specific real-time detection of one single colony-forming unit (CFU), effectively a single bacterium, of *Salmonella* Typhi.[172] In this elegant study, the authors demonstrated the potential of SWNTs to detect the highly virulent *Salmonella* Typhi pathogen at the single-bacterium level. In contrast, classical microbiological tests currently take between 24 and 48 h before a diagnosis for Salmonellosis can be made, because of the need to grow cultures, thus illustrating the strong potential of microbiological diagnostic sensors. Early diagnosis can be life-saving because serious dehydration from diarrhea can lead to death, especially in tropical countries.

3.2. SWNT-Based Field-Effect Transistors

FET-based biosensors represent two important changes compared with electrochemical biosensors: firstly, they use electrical detection, which exploits the changes in resistivity that occur when the molecules of interest adsorb on the FET surface; and, secondly, they are microscale, or even nanoscale, devices. These differences offer some advantages over larger electrochemical devices, as is well illustrated by work from Lieber's research group on FETs made from Si nanowires.[173] In one case, it was demonstrated that label-free, real-time, multiplexed detection of cancer markers can be achieved, while observing, rather remarkably, no significant contribution from nonspecific binding of other proteins.[174] In another study, Lieber and co-workers were able to demonstrate single-virus detection with silicon-nanowire FETs.[175] The excellent performance of such sensors is due primarily to the nanoscale dimensions of the silicon nanowires, which offer high sensitivity, as well as their suitability for biofunctionalization, which provides selectivity. Given the popularity of silicon nanowires for electrical biosensors, it comes as no surprise that SWNTs are also finding increasing use in FET-style biosensors. Besides their inherent nanoscale size and excellent electrical properties, SWNTs are only one molecular layer thick, so, like graphene, every carbon atom is at the surface. Thus, the adsorption of any molecule onto the surface of a SWNT will change the electrical properties of an entire nanotube, therefore making CNT-based sensors capable of extremely high sensitivity[176,177] over a broad range of analytes in gaseous or liquid environments. Indeed, the first single-SWNT biosensing FET was reported by Dekker and co-workers;[45] it was shown that such a biosensor could be capable of measuring enzymatic activity at the level of a single nanotube. Another generic benefit is the robust nature of carbon chemistry, which enables production of reliable, long-lived sensors. Finally, because nanotubes are so tiny, little power is needed to operate the sensors, and multiple nanoscale sensors can be integrated on one small chip, with minimal power and space requirements.

Given these advantages, many research groups have investigated the application of CNT devices to electrically detect biomolecules such as enzymes, proteins, oligopeptides and oligonucleotides; these have included the research groups of Dai,[44] Dekker,[45] Gruner,[178] Tao,[179] Star,[180] and others.[180–182] Some research groups have used single nanotubes as FETs. For example, Dekker and co-workers demonstrated the use of individual semiconducting SWNTs as electrical biosensors for glucose by controlled attachment of the redox enzyme glucose oxidase to the sidewall.[45] Star et al. reported a single-SWNT transistor in which a polymer coating was employed to minimize nonspecific binding, with attachment of biotin to the coating for specific molecular recognition.[178] Tao and co-workers reported the in situ detection of cytochrome c adsorption onto individual SWNT transistors by the changes in the electron-transport properties of the transistors.[179] Other teams have made FETs from random networks of nanotubes. For instance, Star et al.[180] and Li and co-workers[183] have used CNT networks for the detection of DNA hybridization, where the initial strands of DNA are bonded noncovalently to the CNTs. There are benefits to both types of FET geometries, that is, single tubes and tube networks. A single-nanotube device is better able to probe the fundamental sensing mechanism,[36] as its electrical signal does not comprise components from many nanotubes of different sizes and properties. On the other hand, a random network is far easier to fabricate than a FET made from a single tube;[180] furthermore, the FET is more robust and will not cease to function if a single CNT fails.

In the early days of CNT-FET biosensors, the sensing mechanism was not fully understood, and it was thought that possible mechanisms might involve charge transfer from adsorbed species, modifications of contact work-function, substrate interactions, and/or carrier scattering by adsorbed species.[184] More recent analysis has concluded that Schottky-barrier modification and/or charge transfer are the dominant mechanisms responsible for device response.[24,34] Recent work on CNT electrical biosensors has sought ways to increase the specificity of the biosensing process. Tseng and co-workers have used a new approach to ensure specific adsorption of DNA on a CNT transistor array in order to detect DNA hybridization.[185] Their method involved non-covalent attachment of a methacrylate copolymer, which contains ethylene glycol and *N*-succinimidyl groups, to the nanotubes, thereby attempting to limit nonspecific DNA adsorption on the CNTs and simultaneously providing stable binding for DNA probes through robust amide linkages.

Single-cell analysis has become a highly attractive tool for investigating cellular contents. Unlike conventional methods that are performed with large cell populations, this technology avoids the loss of information associated with ensemble averaging. Recent studies have described methods that can quantify specific proteins inside a single cell by means of integrated fluorescence (including confocal microscopy, flow cytometry, and monitoring fluorescent enzymatic products) and, in another instance, by single-molecule imaging.[81,186] These techniques restrict analysis to one or perhaps a few species at a time because of the need to resolve fluorescence from different probes. Moreover, this approach has proven to be difficult, especially in those cases where the cellular environment changes the fluorescence properties of the reporter molecule (e.g., through quenching or resonance energy transfer) or where endogenous fluorescence interferes with the measurements. In contrast to these optical approaches, Sudibya et al. demonstrated that a biocompatible glycosylated nanotube device can interface with single living cells, and electronically detect biomolecular release with high temporal resolution and high sensitivity (Figure 9).[187] By using this in vitro setup, it was possible to record vesicle-mediated exocytosis of catecholamines (i.e., release of stress hormones) into the extracellular space, and hence in the vicinity of the glycosylated SWNTs, thus allowing current changes upon release of the hormones to be recorded. This work is a significant development in the field of cell biology, and opens up new avenues to advance our fundamental understanding of dynamic secretion of biomolecules from single cells, in a similar way to electrochemical strategies for studying single cells.[17] Such an understanding will take us closer towards realizing the exciting potential of these sort of

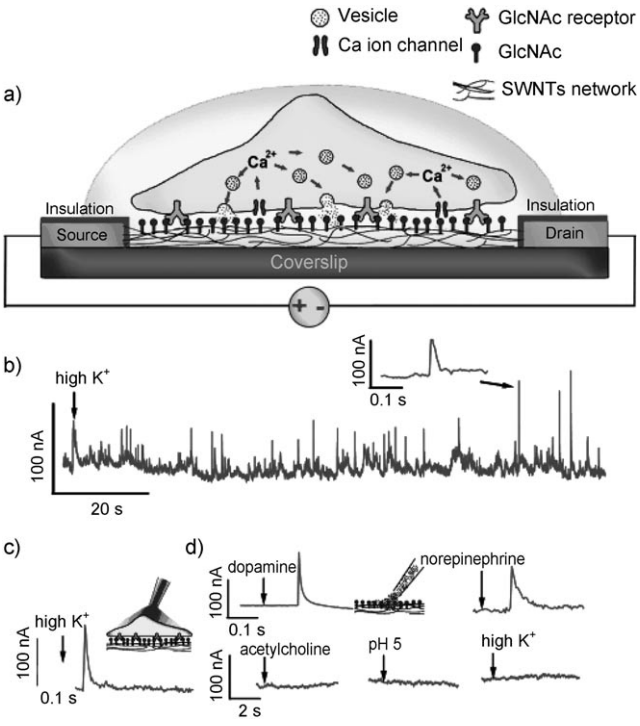

Figure 9. a) Triggered exocytosis and SWNT-network detection. b) Nanotube responses to exocytosis of PC12 cells triggered by high K^+ stimulation. The SWNT network was biased at $V_{ds} = 0.4$ V. c) Stimulation of single PC12 cell through micropipette perfusion of high K^+ solution. d) Transient perfusion of 1 mM dopamine or norepinephrine on glycosylated SWNT-network results in current spikes, while perfusion of acetylcholine, acidic solution (pH 5.0), and a high K^+ ion concentration did not cause appreciable responses. The arrows in (c) and (d) roughly indicate where the stimulations were applied. Reprinted from Ref. [187].

functionalized nanomaterial for "bottom-up" fabrication of functional cell biosensors and associated tailored nanotechnologies. Villamizar and co-workers reported a fast, sensitive, and label-free biosensor that is based on a FET in which a network of SWNTs acts as the conductor channel for the selective determination of *Salmonella* Infantis.[188] Anti-*Salmonella* antibodies were adsorbed onto the SWNTs and subsequently protected with the surfactant Tween 20 to limit nonspecific binding of other bacteria or proteins.

Other types of biofunctionalities further extend the scope of CNT-FET biosensors. So et al. made a screening biosensor device to detect and quantify the number (CFU) of *Escherichia coli* by using aptamer-functionalized SWNT-FETs.[189] The sensors showed a conductance decrease of more than 50% after binding with the *E. coli* bacterium. This biosensor could be life-saving in the rapid diagnosis of *E. coli* borne food poisoning. In another study, the release from living neurons of parathyroid secretory protein chromogranin A, which is often used as a marker for neuroendocrine tumors and neurodegenerative diseases, could be detected by SWNT–FET-based technology.[190] McEuen's research group has used hybrids of supported lipid bilayers and CNTs in the molecular recognition of biological processes that occur at cell membranes.[191] In this study, the conduction of SWNT–FETs was adversely affected by biotin–streptavidin binding. This sort of device could find applications in detecting toxins, such as the cholera toxin, at the membrane level.

3.3. Optical Biosensors Based on CNTs

The number of studies that exploit the optical properties of CNTs for biosensing is small compared with studies that use their electrochemical or electrical properties. However, optical-based systems might be the only way to develop entirely nanoscale biosensors that could operate in confined environments such as inside cells. Such systems typically rely on either: use of the nanotubes on which a classical sandwich-type optical assay is performed;[192] the ability of CNTs to quench fluorescence;[193] or the NIR photoluminescence exhibited by semiconducting nanotubes.[74,194,195] The NIR luminescence of semiconducting SWNTs is particularly interesting for biosensing because NIR radiation is not absorbed by biological tissue, and hence can be used for biosensing within biological samples or organisms.

The ability of CNTs to quench fluorescence has been explored by a number of research groups. A couple of notable examples include work by Yang et al.[196] and Doorn and co-workers.[197] Yang et al. used the preference for single-stranded oligonucleotides to wrap around SWNTs compared with the related duplexes.[196] SWNTs and the sample, which may contain the complementary DNA, were added to oligonucleotides labeled with the fluorophore 6-carboxyfluorescein in solution. If no complementary DNA is present, the fluorescently labeled DNA will wrap around the SWNTs and the fluorescence will be quenched. If the complementary strand of DNA is present in the sample, hybridization with the fluorescently labeled probe DNA will give a rigid duplex that does not wrap around the nanotubes, and hence a fluorescence signal will be observed. The strategy of Doorn and co-workers was somewhat different. They employed a dye–ligand conjugate in which the dye complexed with the SWNTs, thus causing its fluorescence to be quenched.[197] Interaction of the nanotube-bound receptor ligand and the analyte caused the displacement of the dye–ligand conjugate from the nanotubes and the recovery of fluorescence. Such a strategy resulted in nanomolar sensitivity.

Infrared luminescence was used by Strano and co-workers for biosensors in which semiconducting SWNTs are wrapped in double-stranded DNA (dsDNA).[35] The change in conformation of the DNA from its B to Z forms results in a change of the dielectric environment of the SWNTs with a concomitant shift in the wavelength of the SWNT fluorescence. In this initial study,[35] the shift in optical properties upon the change in dsDNA structure was used to detect metal ions that induced such changes in DNA structure. Divalent metal ions of mercury, cobalt, calcium, and magnesium are all known to cause transitions from B to Z in dsDNA and the DNA-wrapped SWNT biosensors were shown to be able to detect all these metals with the sensitivity decreasing in the order $Hg^{2+} > Co^{2+} > Ca^{2+} > Mg^{2+}$. Changes in the structure of dsDNA wrapped around nanotubes has also been exploited for the detection of Hg^{2+} ions by circular dichroism, as the

Hg^{2+} ions are believed to cause a weakening of the DNA–SWNTs interaction, with a resultant decrease in the circular dichroism signal induced by the association of the nanotubes with the DNA.[198]

Wrapping the nanotubes with single-stranded DNA (ssDNA) has also been explored for monitoring DNA hybridization[199,200] and for monitoring small-molecule interactions with the DNA (Figure 10).[47] The latter is a particularly exciting aspect of the earlier study by Strano and coworkers,[35] because it is an extension of the concept to multimodal optical sensing. In this way, Heller et al. simultaneously detected up to six genotoxic analytes, including chemotherapeutic alkylating agents and reactive oxygen species such as H_2O_2, singlet oxygen, and hydroxyl radicals.[47] The ability to detect multiple different analytes on the same sample of ssDNA-wrapped SWNTs is due to the differing optical responses of (6,5) and (7,5) SWNTs. For example, the chemotherapeutic DNA-alkylating agent melphalan causes a red shift in the photoluminescence of both the (6,5) and (7,5) nanotubes; H_2O_2 and Cu^{2+} cause a red shift in the (6,5) band, but no change in the (7,5) band; H_2O_2 and Fe^{2+} damage the DNA, causing an attenuation of both bands, but particularly the (7,5) band. Hence, because of the differing effects of various analytes on the optical signature of a SWNT mixture, chemometric analysis enables multiple analytes to be detected simultaneously. Some sequence specificity was also reported as sequences with more guanine bases are more susceptible to singlet oxygen, while metal-ion responses are greater for DNA sequences with stronger metal binding. The final aspect of this study illustrated the ability of the DNA–SWNTs to detect drugs and reactive oxygen species inside living cells. The DNA–SWNTs had been shown to be able to enter 3T3 fibroblasts by endocytosis without being genotoxic, and retain their photoluminescence.[81] Perfused drugs or reactive oxygen species were observed to induce spectral changes in the SWNTs inside the living cells.[47]

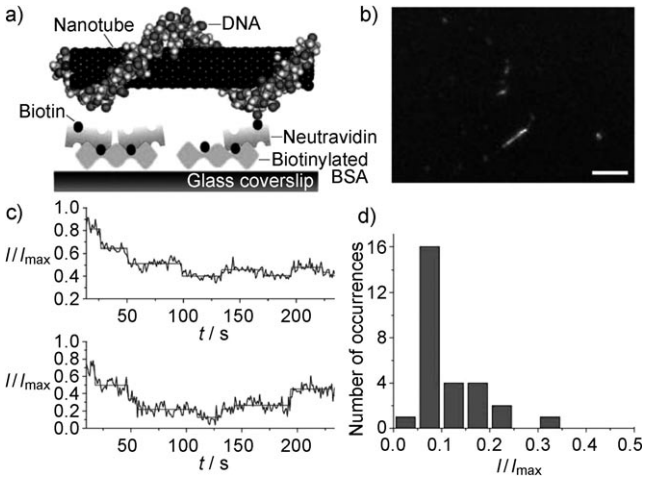

Figure 10. Immobilized DNA–SWNT complexes for the detection of H_2O_2. a) Schematic of DNA–SWNT binding to a glass surface with bovine serum albumin(BSA)–biotin and Neutravidin. b) Photoluminescence micrograph from several DNA–SWNT complexes (scale bar: 10 μm). c) Fitted traces from a NIR movie that show single-step quenching of SWNT emission upon perfusion of H_2O_2. d) Histogram of fitted step sizes from five traces taken from one NIR movie, which allowed the team to conclude they had detected H_2O_2 at the single-molecule level. (Reprinted from Ref. [47] with permission. Copyright 2009 Macmillan Publishers Ltd: Nature Nanotechnology.)

An important feature of using the NIR luminescence of DNA–SWNTs is that it has been reported to be able to detect single-molecule interactions when wrapped either in DNA[36] or collagen,[81] in common with nanotube FET-type devices.[45] In many ways, this system looks almost like the ideal biosensor, as it has nanoscale dimensions and can to detect multiple analytes with exquisite sensitivity in biological media.

4. Graphene-Based Biosensors

Scientifically and technologically, CNTs are a far more mature allotrope of carbon than graphene. This shortcoming is understandable as graphene has only been available for experimental studies since the seminal work of Novoselov, Geim, and co-workers in 2004.[83] Therefore, a brief introduction to the methods for fabricating graphene will be provided here, before examining the research reported to date on graphene-based biosensors.

4.1. Fabrication of Graphene

Any eventual diagnostic applications of graphene-based biosensors will depend on methods for the reproducible fabrication of high-quality graphene in large volumes and for incorporation into sensor devices on an industrial scale. While producing and handling graphene is an extremely active and rapidly moving research field, this overview of the current major approaches to making graphene will show that there is still considerable work to be done.

There are four main approaches to "making" graphene.[201] The first technique is (micro)mechanical cleaving, peeling, or exfoliation of graphite, in which repeated peeling of fragments from high-quality graphite (e.g., HOPG) with pieces of adhesive tape eventually leaves some single layers of graphene.[83] Currently, this method tends to produce the best-quality, least-modified forms of graphene. It can also be refined by putting polymer coatings on the substrate to enhance contrast and increase adhesion of the graphene sheets,[123] thereby allowing production of large pieces of graphene (millimeter-sized pieces are possible these days[96]). However, as the single layers are distributed among many other carbonaceous fragments that can have two, three, dozens, or even hundreds of layers, the challenge in this approach is to identify the fragments of graphene that have the desired number of layers and size. With patience, this method produces high-quality graphene for scientific research, but it is hard to see how it will ever form a high-throughput, large-volume method for the fabrication of graphene.

Methods more amenable to scalable fabrication of graphene often involve wet chemistry. For the most part,

the approach is to exfoliate graphite by converting it into graphene oxide under strongly acidic conditions as described by Park and Ruoff in their recent review (Figure 11a, Method I).[202] This oxidation process creates large numbers of oxygen-containing functional groups, such as carboxyl, epoxide, and hydroxyl groups, on the graphene surfaces. These polar and, in some cases, ionizable groups make graphene oxide extremely hydrophilic and so able to be dispersed into single sheets in water or polar organic solvents. Despite opening up graphene oxide to a world of processing methods, such as spin casting and dip coating, these functional groups cause graphene to lose its unique properties; graphene oxide is an electrical insulator with its layered structure distorted by a large proportion of sp^3 C–C bonds. Therefore, the graphene oxide is typically reduced by means of compounds such as hydrazine (or by heating in a reducing atmosphere) in an effort to regain the structure and properties of graphene. While this process does return much of the conductivity and flatness to the reduced graphene oxide, the final product is not the same as graphene and still contains a significant amount of carbon–oxygen bonds.[130,131,203–205] Provided these differences are understood, graphene oxide and its reduced form both have useful properties in their own rights. However, several research groups have sought to avoid the need for chemical modification by, for example, exfoliating graphite powder in organic solvents of similar surface energies[206] or using a process of intercalation, thermal expansion, and reintercalation to exfoliate graphite and disperse graphene layers into surfactant solutions.[207]

Thermal approaches to growing graphene, although more costly than wet chemical methods, avoid the chemical modification of graphene. As described in recent reviews,[209,210] one approach is epitaxial growth of graphene layers on the basal faces of single-crystal silicon carbide heated to above 1200 °C in an ultrahigh vacuum. The resulting graphene layers, which grow as silicon evaporates from the crystal, tend to show various defects such as substrate-induced corrugations, rotational disorder between the layers, and loops and scattering centers.[211] These effects mean that the electronic bands structures and properties of epitaxial graphene[117,212] differ from those of mechanically exfoliated graphene, so that it is effectively a different material.[209] From this perspective, chemical vapor deposition (CVD) is a better thermal method for graphene growth because it offers more "conventional" properties. Recent efforts have focused on growing really large-scale (e.g., centimeter-sized) films of graphene by passing hydrocarbon vapors over metallic substrates (e.g., Ni or Cu) heated to approximately 1000 °C (Figure 11b, Method II).[208,213,214] Particular benefits of CVD, besides producing macroscale areas of graphene, include the ability to transfer the graphene films to other substrates after dissolving the metallic support (Figure 12). The main challenge is achieving a film with a monodisperse and controlled number of layers, the solution to which is closer since Li and co-workers used Cu substrates for self-limiting growth of graphene films in 2009.[214]

The final approach to fabricating graphene is chemical synthesis, a process in which precursor compounds are combined by organic reactions to form molecular fragments of graphene. The potential of this approach has been explained in several reviews, and full details of the typical reactions used can be found there.[215–217] The thorn in the side of chemical synthesis is that the "graphene fragments" quickly become insoluble as their size increases, so that the final products are limited to pieces of graphene smaller than about 5 nm.[217] It has been shown that controlled deposition and then pyrolysis of arrays of molecules can be used to create larger-scale carbon films,[218] but a true graphene sheet has not been achieved to date. In a radically different approach for chemically creating graphene, Choucair et al. used a solvothermal reaction between sodium and ethanol, followed by rapid pyrolysis, to produce gram-scale quantities of graphene platelets (Figure 11b, Method III).[219]

Clearly, each of the four classes of graphene production methods has its limitations, and none have yet reached the point needed for commercial manufacture of graphene-based biosensors. It also is apparent that a variety of different forms of graphene-like materials can be produced by these methods. These forms offer an even larger diversity of properties for designing biosensors, but also endless opportunities for

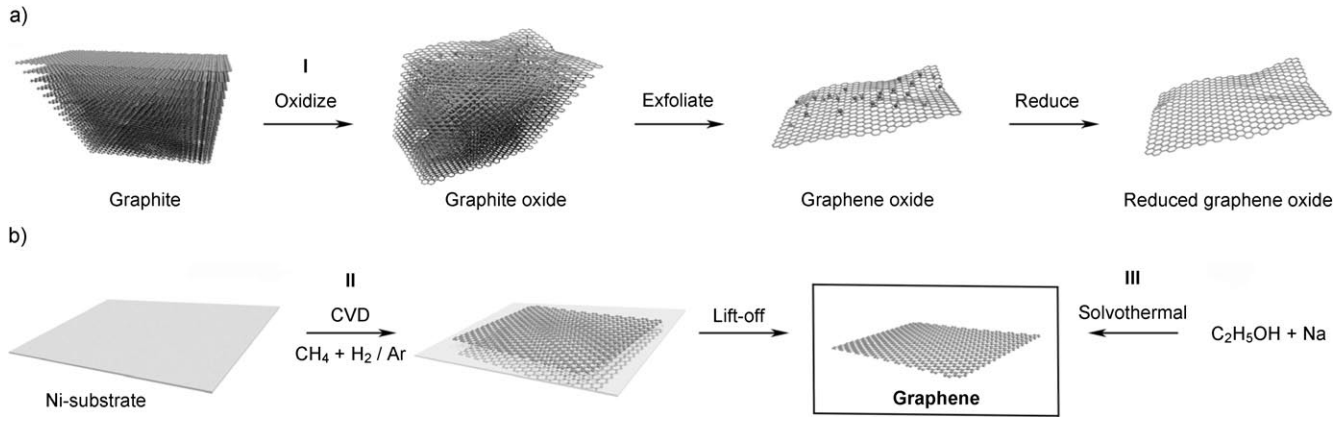

Figure 11. a) The oxidation–exfoliation–reduction process used to generate individual sheets of reduced graphene oxide from graphite (Method I). b) Schematic representation of the approaches to producing graphene by chemical vapor deposition (Method II, left) or by solvothermal reaction (Method III, right).

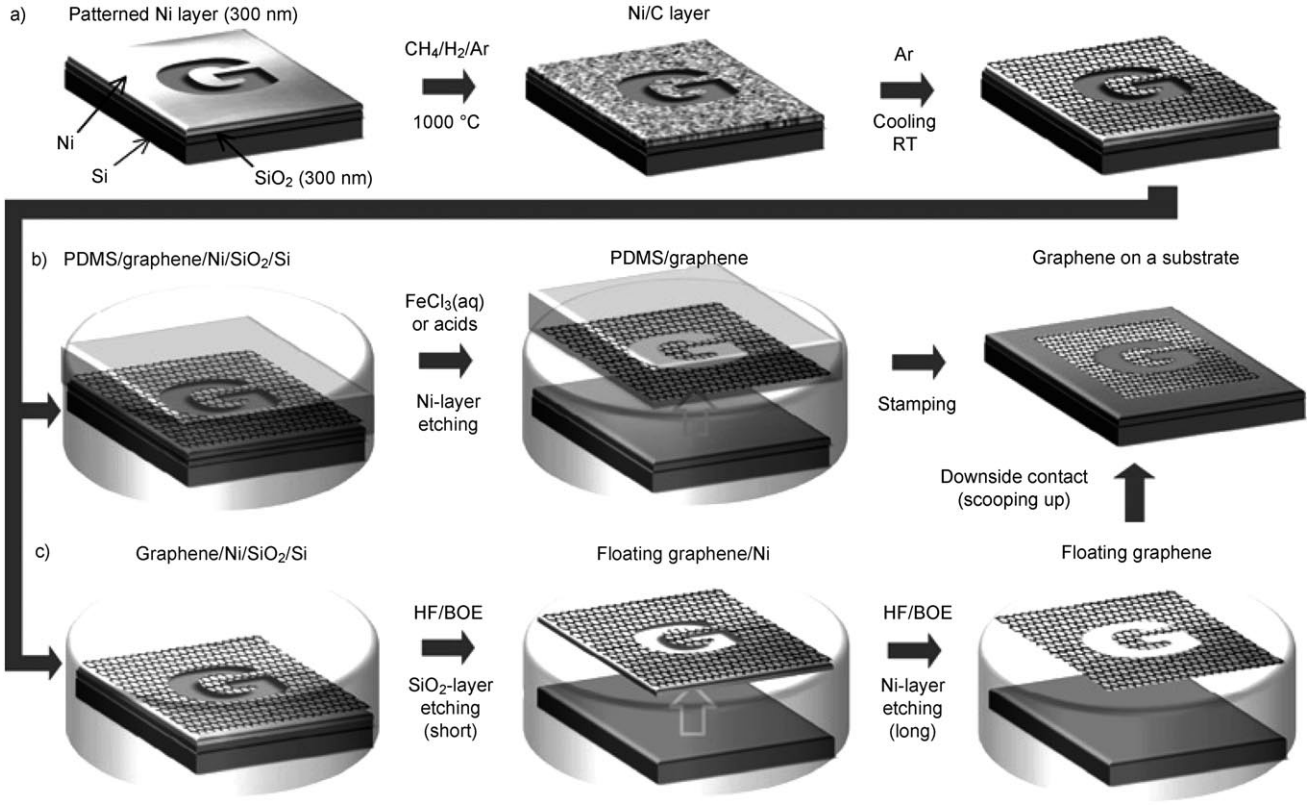

Figure 12. a) Synthesis of patterned graphene films on thin nickel layers by chemical vapor deposition. b) Etching with $FeCl_3$ (or acids) and transfer of graphene films to other substrates by using a polydimethylsiloxane (PDMS) stamp. c) Etching with buffered oxide etchant (BOE) or hydrogen fluoride (HF) solution and transfer of graphene films by "scooping up". (Reprinted from Ref. [208] with permission. Copyright 2009 Macmillan Publishers Ltd: Nature.)

confusion if the materials are poorly characterized and/or inadequately, or simply incorrectly, described when the work is published.

4.2. Graphene in Biosensors

The newness of graphene as a material means that there are relatively few reports of its use in biosensors to date. So, before we examine graphene-based biosensors, it is worthwhile to briefly see what has already been learnt about the sensing capabilities of graphene from other graphene-based sensors. Almost all of these other sensors have been used to detect gases (e.g., H_2O, NO_2, CO, and NH_3), and almost all were electrical sensors that measured changes in resistivity of the graphene, or graphene-derived, sheets during the adsorption of the gas molecules.[134,220–225] Given the range of methods available to make "graphene" and their varying degrees of success (see Section 4.1), it is hardly surprising that more than half of these gas sensors did not actually use pristine single-layer graphene. Even so, several studies have demonstrated that graphene or related materials can exhibit extremely low detection limits for a variety of gases and vapors. For instance, Robinson et al. created an electrical gas sensor,[221] which was based on reduced graphene oxide, and was able to detect toxic gases at levels of parts per billion (ppb). This performance was generally equal to, or substantially better than, the response of sensors made with SWNTs. Comparative measurements showed that reduced graphene oxide films had noise levels that were one to two orders of magnitude smaller obtained with the SWNT-based sensors. Similar, though not as sensitive (parts per million), performance was found for other gas sensors in which reduced graphene oxide was used as the detector.[222–224] In another study, Qazi et al. detected NO_2 at levels as low as 60 ppb by measuring the changes in surface work function, or in electrical conductivity, of flakes of thin graphite.[220] The ultimate in detection, that is, single-molecule detection, was demonstrated by Schedin et al. with highly optimized electrical sensors constructed from few-layer, mechanically exfoliated graphene (Figure 13).[134] After many hours of measuring resistivity changes with their devices in highly diluted NO_2, statistical samplings of gas-molecule adsorption and desorption could be produced, thus showing that those adsorption and desorption peaks were distinct from the zero-mean peak and corresponded to the change in charge that arose from the loss or gain, respectively, of a single electron.

The other central point to emerge from many of these studies, as well as theoretical works,[226–228] was that graphene needs to be functionalized in some way to achieve this impressive gas-sensing performance. Indeed, thermally cleaned graphene shows little or no changes in electrical properties in the presence of certain gases.[225] How then did

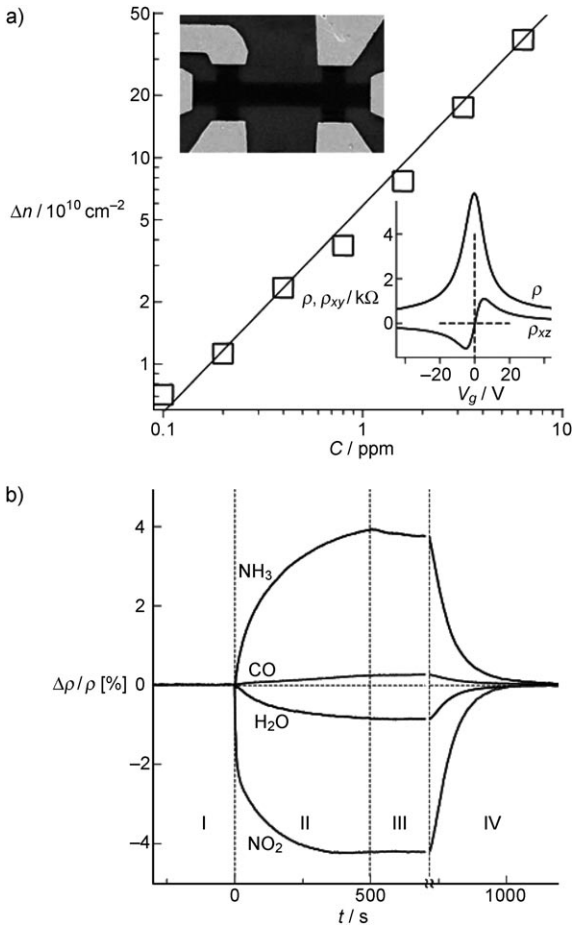

Figure 13. a) Concentration Δn of chemically induced charge carriers in single-layer graphene exposed to different concentrations C of NO_2. Upper inset: SEM micrograph of this device; the width of the Hall bar is 1 μm. Lower inset: the changes in resistivity ρ and Hall resistivity ρ_{xy} of the device with gate voltage V_g. The ambipolar field effect is clearly illustrated. b) Changes in resistivity at zero magnetic field as caused by graphene's exposure to different gases diluted in a carrier gas (He or N_2) to a concentration of one part per million. (Reprinted from Ref. [134] with permission. Copyright 2007 Macmillan Publishers Ltd: Nature Materials.)

Schedin et al. manage to achieve single-molecule detection with "pure" graphene?[134] The answer is that their devices were unintentionally "functionalized" by the residual polymer layer from the lithographic resist, which served to help concentrate the gas molecules and possibly enhance charge transfer. This finding was confirmed by recent experiments in which the electrical gas-sensing performance of graphene devices was compared before and after the polymer resist was removed: without the polymer layer, there was a decline in sensitivity of one or two orders of magnitude, depending on the gases used.[225] Ab initio studies of gas adsorption onto graphene also corroborate the role of impurities or vacancies, thus demonstrating stronger gas adsorption at sites of atomic substitutions or defects.[227,228] The success of reduced graphene oxide gas sensors also supports the importance of functionalization, because those sensors are "functionalized" by the oxygen-containing moieties and defects introduced during oxidation of the parent graphite, and by the nitrogen-containing groups and/or vacancies created by subsequent reduction of the graphene oxide. Experimentally, changing the degree of reduction alters the sensor response, and these impurities and defects appear to be sites of strong (i.e., high-energy) gas adsorption,[221] which is consistent with the modeling studies. Of course, more detailed experiments are needed to untangle the relative contributions to sensor performance that arise from the impurities and defects created by oxidation and, later, by reduction, as well as those that arise from the corresponding changes in electrical conductivity of the sheet and the proportion of sp^2 sites available for low-energy adsorption. Cumulatively, all of this work reveals just how sensitive the performance of devices is to the purity and structure of the graphene, therefore emphasizing the need to take great care in understanding the exact chemistry of the material that is used in sensors.

When focusing on graphene-based biosensors, it is noteworthy that only one of the sensors demonstrated so far has actually incorporated pure graphene;[229] the remainder have employed graphene oxide (and its derivatives)[100,104,230,231] or multilayer graphene and related structures.[97,99,103] We do not wish to detract from these other efforts in any way, but simply wish to emphasize the range of graphene-like materials that have been incorporated into biosensors. The high proportion of work with "modified" forms of graphene is likely to continue into the future because departures from "ideal" graphene obviously offer increased scope for tailoring properties when designing biosensors. For example, the use of two or more layers of graphene opens up the ability to hone graphene's electronic properties, while surface functionalization, whether by covalent or physical modification, can be used to increase sensitivity and/or selectivity and to minimise nonspecific binding.

Most biosensors reported to date have used electrochemical reactions involving various types of "graphenes" to detect biomolecules. For instance, Lu et al. have created graphitic electrode materials for sensitively measuring glucose concentration.[97,103] The electrodes were nanocomposite films of thermally exfoliated graphite "nanoplatelets" dispersed in the conductive polymer Nafion, and are reminiscent of similar electrodes fabricated with powdered graphite or CNTs. The nanocomposites of nanoplatelets and Nafion exhibited significant oxidation and reduction currents in H_2O_2 solution, whereas a Nafion-modified gold electrode had negligible electrochemical response, thus showing that the graphite nanoplatelets catalyzed the oxidation and reduction of the H_2O_2 and lowered the overpotential to detect the peroxide, relative to Nafion–gold electrodes. Similar trends have been observed for CNT electrodes.[232] The addition of glucose oxidase to the nanocomposites produced electrodes that respond to glucose up to three times better than most sensors made with CNTs.[97] In a subsequent publication, the same research group reported the precipitation of catalytic platinum or palladium nanoparticles onto the graphite nanoplatelets, which kept the nanoparticles extremely small and, in the case of platinum, evenly distributed. Composite electrodes made from the nanoparticle-decorated nanoplatelets and Nafion had exceptionally high surface-area-to-volume ratio for these costly metals, thus offering outstanding perfor-

mance, with a marked decreased in the overpotential needed to detect H_2O_2, at low cost. This kind of approach has been used extensively for CNTs, where the nanotubes similarly provide a high surface area for growth of catalytic nanoparticles.[157,233]

A different approach to glucose detection was attempted by Shan and co-workers, who made electrodes from reduced graphene oxide "protected" with polyvinylpyrrolidone, from a polyethylenimine-functionalized ionic liquid and glucose oxidase.[104] A key aim of their study was to exploit the high surface area and moderate electrical conductivity of reduced graphene oxide to attempt direct electron transfer between the glucose oxidase and the electrode. Like many studies in this field, however, the question remains as to whether the observed redox peaks of the electrochemistry observed were genuinely from flavin adenine dinucleotide (FAD) sitting in its native configuration deep within glucose oxidase, or merely from a denatured form of the enzyme. It is unclear if or how the reduced graphene oxide might have mediated direct electrochemical communications between the redox-active enzyme and the electrode used in this study.

Other research groups have explored how the edges of multilayer graphene nanoflakes[99] or the edges and functional groups of reduced graphene oxide[100] perform at electrochemically detecting important neurotransmitters like dopamine and serotonin. In 2008, Shang et al. used microwave-plasma-enhanced CVD to grow multilayer graphene nanoflake films on Si substrates, without the use of any catalysts.[99] The resulting films comprised multilayer nanoflakes with exposed sharp edges that can undergo redox reactions in solution and, therefore, detect electrochemically active biomolecules. Exposed edges that facilitate electrochemistry is consistent with active electrochemistry observed for edge-plane sites on HOPG[60] and the tips of CNTs.[62] Cyclic voltammetry measurements with a graphene nanoflake electrode showed clear voltammetric peaks for the direct oxidation of dopamine in solution. Clear peaks were also observed for ascorbic acid (vitamin C) and uric acid, which are potentially interfering molecules, when analyzed in separate solutions. Crucially, these peaks remained well-resolved in a mixed solution of the three compounds, thus showing that the nanoflake electrodes could be used to to clearly identify dopamine in mixtures (Figure 14). This result contrasted with the response of a glassy carbon electrode, in which the biomolecules showed similar broad peaks at higher potentials, whether analyzed individually or in mixtures. Similar effects have been observed previously in electrochemical studies with electrodes that incorporate CNTs.[234,235] The stark contrast in performance of the two electrodes demonstrated the faster electron-transfer kinetics and favorable electrocatalysis provided by the defects at the edges of the graphene nanoflakes.

In the more recent study, Alwarappan et al. compared the electrochemical properties and sensitivity of reduced graphene oxide sheets with SWNTs.[100] Cyclic voltammetry measurements were made in solutions of dopamine and of serotonin by using electrodes covered in either of the different carbon structures. For both types of biomolecules, the electrodes covered in reduced graphene oxide showed

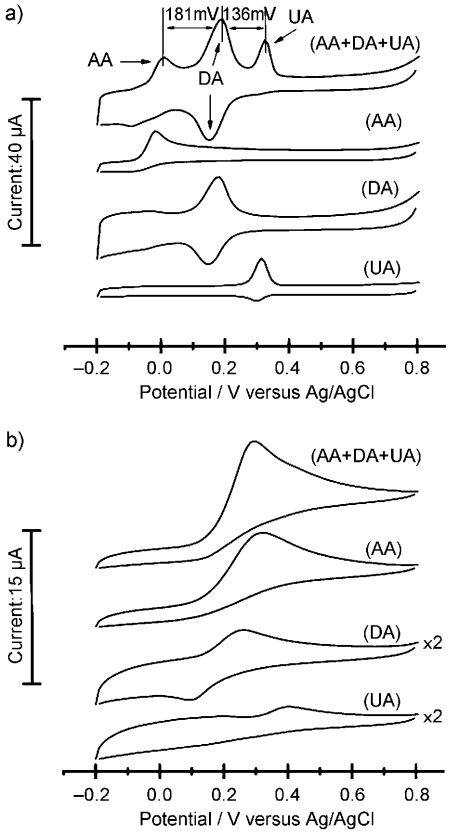

Figure 14. Cyclic voltammetry of the a) nanoflake and b) glassy carbon electrodes in solutions containing 1 mM ascorbic acid (AA), 0.1 mM dopamine (DA), and/or 0.1 mM uric acid (UA). Reprinted from Ref. [99].

greater currents at lower potentials, as well as higher electrode stability, than the electrodes covered in nanotubes. Furthermore, the reduced graphene oxide electrode was able to resolve three distinct oxidation peaks in a solution of dopamine, serotonin, and ascorbic acid, whereas the latter electrode showed only a single broad peak. The greater sensitivity, stability, and signal-to-noise ratio of the graphene oxide electrodes seemed to be due to the high concentration of edge and surface defects available for electrochemical reactions, in comparison with the few active sites on the SWNTs.

The first graphene-based electrical biosensors were demonstrated by Mohanty and Berry, who produced sensors from graphene oxide or from graphene amines made by treating graphene oxide with nitrogenous plasmas or ethylenediamine.[230] These few-layer graphene derivatives were adsorbed from a suspension onto silica surfaces of opposite charge. While this procedure electrostatically anchored the sheets to the silica, it also created large wrinkles in them. Gold electrodes were made above or below the flakes to allow for subsequent electrical measurements. Not surprisingly, the electrical measurements showed that the chemically modified graphene sheets were *p*-type semiconductors with high resistances (on the order of megaohms) and extremely low carrier mobilities ($0.002–5.9\ cm^2 V^{-1} s^{-1}$). Mohanty and

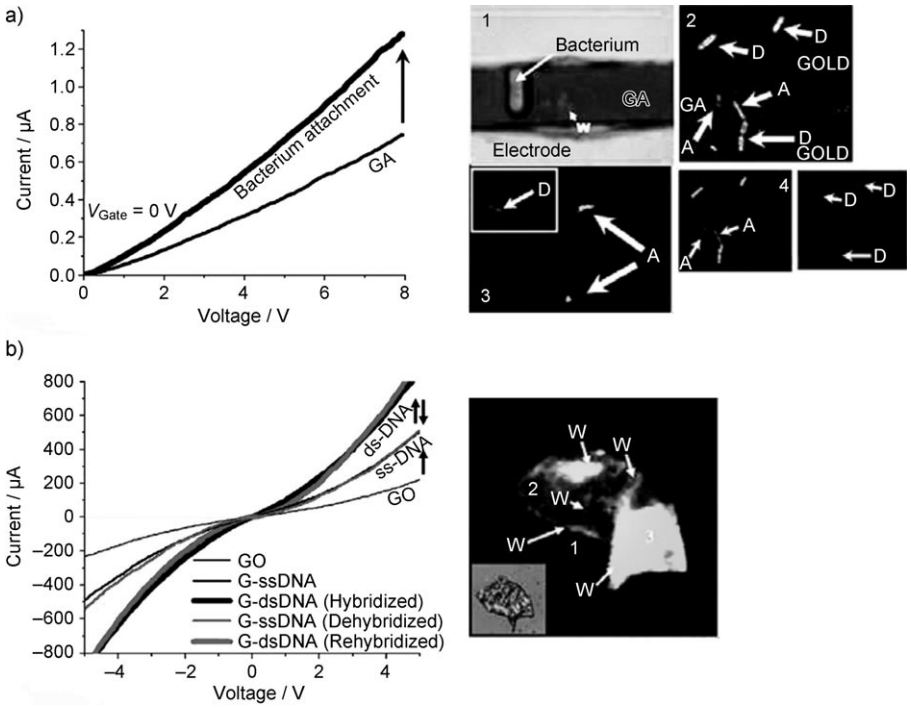

Figure 15. The electrical response of a) graphene amine GA to a single bacterium (the device is shown in inset 1) and b) graphene oxide GO to grafting of DNA, ss-DNA, and subsequent hybridization of the DNA with the complementary strands, ds-DNA. ss = single-stranded, ds = double-stranded. (Reprinted from Ref. [230] with permission. Copyright 2008 American Chemical Society.)

Berry[230] then exploited the functional groups on graphene oxide or graphene amine to create biosensors. For example, single-stranded oligonucleotides were chemically grafted to the graphene-derivatives, and then the fluorescence was monitored as rhodamine-green-tagged complementary oligonucleotides hybridized with the tethered strands. Electrical measurements showed that the initial tethering of single DNA strands more than doubled the conductivity of the graphene oxide (Figure 15). This result was attributed to the negatively charged molecules providing negative gating, which increased the hole density. DNA hybridization caused a further increase in conductivity, which was completely reversible during cycles of denaturing and rehybridization. In another experiment, it was shown that negatively charged bacteria could be electrostatically adsorbed on the positively charged graphene amine, where they survived for up to 4 h. Electrostatic adsorption of a single bacterium on a graphene–amine device caused a 42% increase in conductivity, thus demonstrating single-cell sensitivity. Finally, it was shown that adsorption of polyelectrolyte molecules on the modified graphenes caused polarity-dependent changes in electrical conductivity.

A very recent study by Ohno et al. demonstrated electrical detection of dissolved bovine serum albumin (BSA), by means of an electrolyte-gated graphene FET.[229] The sensor was produced from mechanically exfoliated single-layer graphene onto which metal contacts were deposited lithographically; consequently, the transducer was virtually ideal graphene, except for any residual polymer resist from the lithography. Supported on a SiO_2-capped silicon wafer, and with an electrolyte solution and reference electrode above, the sensor could be doped electrically by applying voltages to either the bottom gate (the doped silicon) or the top gate (the reference electrode). In this way, the authors were able to explore the changes in conductance of the device with different top- or bottom-gate voltages, as well as with different pH values. The position of the neutrality point (the minimum conductivity, which corresponds to the Dirac point) increased linearly over the range of pH values examined, from 4.0 to 8.2. This sensitivity of graphene's electrical properties to solution pH is consistent with an earlier study on epitaxial-graphene devices,[98] and suggests that graphene might find future applications in measuring pH. Ohno et al. then examined the electrical response of their sensor to adsorption of BSA protein from standard solutions.[229] Step changes in conductance with sequential additions of increasing amounts of BSA were observed, and the protein could be detected at levels as low as 0.3 nM. While future sensors clearly will require functionalization of the graphene to ensure specificity and minimize nonspecific binding, this study definitively confirms the potential of pristine graphene for detecting biomolecules, in the same way that the seminal work of Schedin et al.[134] showcased graphene's capacities for sensing gas molecules.

Finally, Lu et al. have developed an optical approach to sensing DNA fragments and proteins in solution by exploiting quenching of fluorescent tags during adsorption of biomolecules on graphene oxide.[231] By recognizing that nucleobases of DNA weakly bind to graphene oxide and reduced graphene oxide,[236] the researchers speculated that fluorescently tagged oligonucleotides would bind to graphene oxide flakes and, in so doing, their fluorescence would be quenched.[231] This concept was confirmed when the presence of graphene oxide quenched 97% of the fluorescence signal from the single-stranded DNA. As hoped, the subsequent addition of the complementary strands of DNA caused hybridization, displacing the tagged DNA from the graphene oxide surfaces and restoring approximately 77% of the original fluorescence signal. Obviously, this approach is analogous to the fluorescence-quenching approaches involving CNTs that have already been described (Section 3.3).

5. Carbon Comparisons

We posed three quite critical questions at the very start of this Review and now, having examined the latest in biosensors made with CNTs or graphene, can set about answering them.

5.1. What Kinds of Advantages Do Carbon Nanomaterials Offer over Macroscopic Materials for Making Biosensors?

As is evident from the above discussion, carbon nanomaterials certainly offer significant advantages in the construction of biosensors. For the sake of brevity, we will outline two main examples here. The first is the unique, but perhaps not fully understood, electrochemical properties of carbon nanomaterials. A good example is the ability to electrochemically identify and quantify the concentrations of mixed biomolecules, such as dopamine and serotonin, and interfering molecules, such as ascorbic acid and uric acid, which are indistinguishable with conventional glassy carbon electrodes (see Section 4.2).[99,100,234,235] It also is noteworthy that these latter acids, which are strong antioxidants, also show distinctive, but often unseen, concentration changes in a variety of medical conditions, thus adding further diagnostic value to the distinct, high-sensitivity electrochemical peaks available with CNT or graphene electrodes. Other advantages of CNTs for biosensors include their ability to act as efficient ion-to-electron transducers in potentiometric analysis,[237,238] or the fact that SWNTs, with their small size and high conductivity, can also be used as the smallest possible electrodes, which are comparable to the size of single biomolecules.[239] Their small sizes and electrochemically active tips also make SWNTs able to "plug into" larger biomolecules to access internal redox sites (see Section 3.1).

The second advantage is the outstanding electrical properties of carbon nanomaterials. When appropriately made, SWNTs and graphene can show ballistic transport with extremely high electron mobilities that offer unprecedented opportunities for high-speed sensors (see Sections 2.1 and 2.2). Moreover, both materials have every atom in their structures exposed on their surfaces, so even small changes in the charge environment caused by the adsorption of biomolecules can give measurable changes in their electrical properties. Indeed, the ability to detect biomolecules[45] and gas molecules[134] at the single-molecule level, as well as single cells[187,230] with CNTs and graphene (or related materials) has already have demonstrated (see Sections 3.2 and 4.2).

One disadvantage, however, is that carbon nanomaterials are not easy to handle and are rather heterogeneous in nature—at least at present. This disadvantage means their application in biosensors should be limited to devices where their advantages are truly needed and therefore outweigh their limitations.

5.2. Does Graphene Offer Any Genuine Advantages over CNTs for Making Biosensors?

This is a more difficult question to answer because of graphene's relative youth as a material, and because there have been few head-to-head comparisons of the relative performance of CNTs and graphene in biosensing, and certainly none in completely optimized systems. Nevertheless, there are important differences in properties that suggest that graphene might well have some advantages over CNTs for certain types of sensors. Two main classes of evidence can be provided here. The first relates to the way that graphene addresses some of the problems that limit the application of CNTs in biosensors. For example, the high-aspect-ratio, one-dimensional nature of CNTs, which is so useful in many ways, makes it difficult to controllably assemble nanotubes to make complex sensors or other devices. As one research group put it: "Unfortunately, incorporation of nanotubes in large-scale integrated electronic architectures proves to be so daunting that it may never be realized."[209] In contrast, graphene, though still not "out of the woods" in terms of production methods (see Section 4.1), is highly amenable to microfabrication. Indeed, ever since the first experimental study on graphene,[83] researchers have used traditional microfabrication approaches—such as masking, electron-beam lithography, oxygen-plasma dry etching, and metal deposition—to fabricate devices from, for example, mechanically cleaved graphene,[83] reduced graphene oxide,[203] epitaxially grown multilayer graphene,[212] and vapor-deposited graphene.[208] One can even bypass the exfoliation stage altogether by carrying out the lithography directly on graphite (HOPG) and transfer printing the patterned graphene to the desired substrate, as recently shown by Song et al.[240] Another example of a limitation that graphene overcomes is the almost inevitable metallic impurities present in CNTs[58,61] (see Section 2.1), which, at the very least, confound the nanotubes' performance in biosensors. Mechanically exfoliated graphene and some types of vapor-deposited graphene are entirely free from these catalytic impurities, thus simplifying graphene's intrinsic electrochemistry and potentially offering more reproducible sensing response.

The second class of evidence for the probable advantages of graphene involves aspects of its performance that are superior to those of sensor materials in general. A particular strength of graphene in FET-style sensors, for example, is the quality of its crystal structure and band structures, which result in uniquely low noise levels. Its high conductivity means that it is subject to low levels of thermal noise, while its atomic structure contains few defects so that $1/f$ noise (also known as "pink noise") is low.[134] Besides its inherent crystalline quality, graphene's electrical noise can be further reduced by adjusting the number of layers to produce a band structure that better screens against variations in potential because of external impurities.[221,241] Adjusting the number of layers also affords other benefits, such as the ability to electrically tailor the band gap in bilayer graphene[108] in order to maximize detection sensitivity. Further reductions in noise, and therefore improvements in sensitivity, might also be possible through minimizing substrate effects and improving the quality of electrical contacts to the graphene.[242] Other outstanding properties of graphene include its high flexibility,[208] which is required for mechanically robust sensors, and its high transparency.[207,208] The Raman and infrared activity of graphene[84,88] and the sensitivity of these properties to impurities, defects, or strains[127,128] also suggest we might see larger numbers of future biosensors based on optical principles. However, graphene lacks the diversity of optical response shown by different chiral forms of CNTs (perhaps best illustrated by the work of Heller et al.[47] presented in Section 3.3) as well as the structural rigidity of CNTs, so that

nanotubes might prove best for developing intracellular optical sensors in the long term.

5.3. What Insights from Research in CNT-Based Biosensors Can Inform Further Development of Graphene-Based Biosensors?

The biggest, and perhaps the most important, point we can learn from CNT-based biosensors that is of direct relevance to graphene is just how sensitive biosensor performance is to the exact structure and chemistry of the carbon nanomaterial. One of the main reasons for the dramatic differences in the properties of CNTs and their performance in sensing applications is that the term "carbon nanotube" covers a plethora of different materials. Beside the obvious differences between SWNTs and MWNTs, even supposedly similar batches of nanotubes have different lengths and structures, electronic types, purities, modifications, and levels of agglomeration. This point is really critical because these differences are the cause of much confusion, and much of the variation in the CNT literature. The vast spectrum of different results obtained from apparently the same experiments in electrochemical systems is perhaps the best example of this (see Section 2.1). The moral of the story is the need for detailed characterization of carbon nanomaterials, and for great care and precision in how the materials are named.

When it comes to graphene, we cannot emphasize enough that this moral is equally true. Even for relatively idealized graphene, its electrical and optical properties are highly sensitive to factors that include the number of layers, the substrate, impurities and contaminants, and the edge structure and chemistry (see Section 2.2). When one adds the further differences in structure and chemistry that are made possible by the diverse fabrication methods (see Section 4.1), especially around graphene oxide and its reduced forms, the potential for material variability seems daunting. As with CNTs, all these sources of variability offer scope for tremendous variations in measured performance of "graphene" and commensurate potential for an equally confused account of the material and its performance in biosensors. The literature is becoming dotted with works that use the term "graphene" relatively indiscriminately to describe what are effectively different materials and sometimes even graphite. Therefore, we suggest that, as a matter of some urgency, there is a need to develop a common, agreed, and precise terminology for the various forms of graphene. At the very least, we feel authors should refer to 1) the origin of the material and 2) the number of layers: for example, single-layer graphene, bilayer graphene oxide, chemically reduced few-layer graphene oxide and so on, although a better, and more systematic, naming system might emerge.

6. Summary and Outlook

It is worth reiterating again that we did not intend this Review to cover the entire literature on carbon nanomaterials, and their multifaceted nature, properties, and applications across fundamental and applied sciences. Instead, we have focused on their potential to act as effective biosensors. Even then, of the large number of papers available, we have still been selective, and have chosen only papers that we felt have had substantial impact for biosensors, or have genuine potential for future applications. For example, a detailed search for "carbon nanotubes and biosensors" in the biomedical database *PubMed* reveals 418 original research papers and 36 reviews since 2002, whereas "graphene and biosensors" resulted in only seven research papers and no topical biosensor reviews, thus illustrating the early days of the field and the timely nature of this Review. In closing, we will briefly outline some of the key challenges that still remain for continued development of biosensors made from CNTs or graphene, and then present some ideas on the future directions in this broad field.

Despite their promise, both graphene and CNTs still face considerable challenges. Probably the most severe drawback for the application of SWNTs is heterogeneity. While numerous approaches have been taken for the separation of semiconducting and metallic tubes from as-synthesized samples,[48,145,243–245] problems remain as post-synthesis separation processes are often tedious and even involve possible contamination or degradation of nanotubes. An alternative approach is to manipulate the electronic properties of SWNT through covalent chemical functionalization,[246] although this method disrupts the π bonding by converting some atoms into sp^3-hybridized carbon atoms.[247] Consistent fabrication is an equally great challenge for graphene, as illustrated in Section 4.1. Mass production of consistent and reproducible sensors from either type of material is still some way off.

The two-dimensional nature of graphene brings other challenges, which include: separating the layers and keeping them separated, if isolating graphene from graphite, to control the number of layers; minimizing folding and bending during processing; and limiting substrate effects, which are exacerbated by graphene's tendency to adhere strongly to various substrates.[213] Avoiding surface contamination is a particular challenge. Graphene is highly lipophilic (or hydrophobic) and so invariably has adsorbed contaminants, particularly hydrocarbons, on its surface;[91,92,248,249] this effect is exacerbated by graphene's high lateral surface area. Certain types of processing introduce more contaminants. For instance, resists used in lithography and microfabrication of graphene are difficult to remove.[248] Likewise, solvents used for exfoliating and casting graphene films tend to leave a substantial residue.[206] While these residues can be removed by moderate-temperature annealing under vacuum or reducing atmosphere, the challenge is preventing undesired contaminants—as opposed to intended functionalization—that deposit during use of graphene devices and thereby alter graphene's properties and ultimately its response in biosensors.

Given the complications that arise from the heterogeneous nature of CNTs, recent (and continuing) advances in the synthesis and purification of CNTs undoubtedly will advance our understanding of these materials and, therefore, will increase their usefulness in biosensors. The same will be true for graphene as research into synthesis, purification, modification, and biofunctionalization continues to acceler-

ate, as was recently reviewed by Geim.[96] In the case of CNTs, for example, controlled microwave treatment of CNTs can remove over 90% of the iron catalyst present,[250] but the presence of residual iron greatly affects their electrochemical properties. Methods for separating the different chiral, and hence conductive, forms of CNT are also being developed, based on reports that aromatic polymers (polyfluorenyl-based) selectively wrap around the large-diameter CNTs as well as the (6,5)-chiral form of CNTs.[251]

In terms of the outlook for biosensors based on carbon nanomaterials, some indications of future directions are evident from recent reports that, while not strictly about biosensors, provide knowledge and insights that will advance the design of future sensor devices. Gheith et al., for example, reported the stimulation of neural cells by lateral currents in highly conductive SWNT multilayers.[252] This effect has potential in a future biomedical device in which electrically responsive cells (such as muscle or endocrine cells) can be studied at the single-cell level; and, when combined with drug studies, this device can act as a "pharmacological sensor" at the molecular level. Fadel et al. used the high surface area of SWNTs to present high local concentrations of anti-CD3 (i.e., primary antibodies generated against the T lymphocyte cell receptor) to T lymphocytes in order to provoke an enhanced T cell immune response.[253] This response is not only directly important within potential medical settings—the high-density presentation of protein stimuli is key for inducing an effective immuno-mediated cellular response to cancers, for instance—but also as an indirect "systemic biosensor" that one day might be used to monitor the immune response in immune-deficient patients. By taking this principle one step further, other workers have functionalized SWNTs with cancer antibodies, and then used the modified nanotubes for thermal ablation of tumor cells.[254] This novel approach exploits the heating of SWNTs when they absorb energy from NIR light, to which tissue is relatively transparent. The technique is also promising for a precisely selective treatment because the antibody-functionalized SWNTs only target the cancer cells and then, upon NIR irradiation, kill those cells by localized heating (hyperthermia). Another future prospect for biosensing might be the use of MWNTs coupled to atomic force microscopy (AFM) tips. This technique will allow delivery of molecular "cargo" by force-mediated nanoinjection within the cells' interiors.[255] When tagged with antibodies, such nanotube tips have the potential to probe and analyze subsets of cells (malignant, differentiated, etc.) at a resolution better than laser optical techniques, while the use of nanotube tips treated with different antibodies on microarray AFM tips will allow researchers to go "fishing for molecules" in a multiplexed fashion.

In conclusion, it is clear that carbon nanomaterials offer many advantages for the detection of biomolecules, and continued development of these technologies will be a particular boon to clinical laboratory science. Carbon-based sensor technology is not only relatively cheap to produce, it is also lightweight and compact and hence we expect to see commercial developments in "compact carbon chemistry", analogous to the "dry chemistry" wave that medical pathology has been through in recent years. Indeed, miniaturization and production of compact biosensors as diagnostic devices is a thriving research and development area, and the potential applications are countless. Examples include robust diagnostic devices for emergency use in remote areas far away from comprehensive medical facilities; low-cost sensors to detect pollutants in natural environments such as waterways; rapid, on-the-spot health-monitoring devices for use during space travel; ubiquitous yet unobtrusive detectors in high-risk buildings in order to counter bioterrorism by the quick detection of viral and bacterial pathogens; self-monitoring biological implants for those with serious health conditions; and devices integrated into the equipment of defense-force personnel to provide immediate detection of biological or chemical warfare agents. Realization of these and other biosensor applications will serve to protect lives, improve health, and better preserve the environment. Undoubtedly, graphene will play a key role in the biosensors of the future because of its many unique properties, and because, as a two-dimensional sheet, it is amenable to existing microfabrication techniques and to large-area biofunctionalization. Despite the possibilities, however, we must finish with a word of caution: as is widely agreed among scientists, considerable work must still be done to assess, and optimize, the biocompatibility of carbon nanomaterials, and to determine any possible toxicity and health risks they might have during long-term use.

The authors acknowledge the facilities and technical assistance from staff at the Australian Key Centre for Microscopy and Microanalysis (AKCMM), the University of Sydney. W.Y. is a recipient of a University of Sydney Postdoctoral Fellowship (U2158PJ-2007/2010). This work was supported in part by the Australian Research Council (P.T., J.G., and F.B.) and the ARC/NHMRC FABLS research network (RN0460002) (W.Y., P.T., and F.B.).

Received: June 26, 2009
Revised: October 6, 2009
Published online: February 24, 2010

[1] W. R. Yang, P. Thordarson, J. J. Gooding, S. P. Ringer, F. Braet, *Nanotechnology* **2007**, *18*, 412001.
[2] L. Agui, P. Yanez-Sedeno, J. M. Pingarron, *Anal. Chim. Acta* **2008**, *622*, 11.
[3] M. Pumera, S. Sanchez, I. Ichinose, J. Tang, *Sens. Actuators B* **2007**, *123*, 1195.
[4] D. R. Thévenot, K. Toth, R. A. Durst, G. S. Wilson, *Biosens. Bioelectron.* **2001**, *16*, 121.
[5] P. Bergveld, *IEEE Trans. Biomed. Eng.* **1970**, *BME-17*, 70.
[6] Y. Cui, Q. Q. Wei, H. K. Park, C. M. Lieber, *Science* **2001**, *293*, 1289.
[7] J. J. Storhoff, R. Elghanian, R. C. Mucic, C. A. Mirkin, R. L. Letsinger, *J. Am. Chem. Soc.* **1998**, *120*, 1959.
[8] W. R. Yang, J. J. Gooding, Z. C. He, Q. Li, G. N. Chen, *J. Nanosci. Nanotechnol.* **2007**, *7*, 712.
[9] J. J. Gooding, F. Mearns, W. R. Yang, J. Q. Liu, *Electroanalysis* **2003**, *15*, 81.
[10] J. J. Gooding, *Electroanalysis* **2008**, *20*, 573.
[11] A. Heller, *Acc. Chem. Res.* **1990**, *23*, 128.
[12] P. V. Bernhardt, *Aust. J. Chem.* **2006**, *59*, 233.
[13] J. Wang, *Electroanalysis* **2007**, *19*, 769.

[14] F. Patolsky, G. F. Zheng, C. M. Lieber, *Anal. Chem.* **2006**, *78*, 4260.
[15] J. Wang, *Chem. Rev.* **2008**, *108*, 814.
[16] I. Willner, M. Zayats, *Angew. Chem.* **2007**, *119*, 6528; *Angew. Chem. Int. Ed.* **2007**, *46*, 6408.
[17] C. Amatore, S. Arbault, M. Guille, F. Lemaître, *Chem. Rev.* **2008**, *108*, 2585.
[18] C. X. Yu, J. Irudayaraj, *Anal. Chem.* **2007**, *79*, 572.
[19] O. A. Sadik, A. O. Aluoch, A. L. Zhou, *Biosens. Bioelectron.* **2009**, *24*, 2749.
[20] M. Stromberg, T. Z. G. de La Torre, J. Goransson, K. Gunnarsson, M. Nilsson, P. Svedlindh, M. Stromme, *Anal. Chem.* **2009**, *81*, 3398.
[21] K. E. Sapsford, T. Pons, I. L. Medintz, H. Mattoussi, *Sensors* **2006**, *6*, 925.
[22] J. M. Pingarron, P. Yanez-Sedeno, A. Gonzalez-Cortes, *Electrochim. Acta* **2008**, *53*, 5848.
[23] B. He, T. J. Morrow, C. D. Keating, *Curr. Opin. Chem. Biol.* **2008**, *12*, 522.
[24] D. R. Kauffman, A. Star, *Chem. Soc. Rev.* **2008**, *37*, 1197.
[25] K. Maehashi, K. Matsumoto, *Sensors* **2009**, *9*, 5368.
[26] Rajesh, T. Ahuja, D. Kumar, *Sens. Actuators B* **2009**, *136*, 275.
[27] K. A. Kilian, T. Boecking, J. J. Gooding, *Chem. Commun.* **2009**, 630.
[28] H. L. Qi, Y. Peng, Q. Gao, C. X. Zhang, *Sensors* **2009**, *9*, 674.
[29] A. K. Sarma, P. Vatsyayan, P. Goswami, S. D. Minteer, *Biosens. Bioelectron.* **2009**, *24*, 2313.
[30] P. M. Ajayan, *Chem. Rev.* **1999**, *99*, 1787.
[31] I. Heller, J. Kong, H. A. Heering, K. A. Williams, S. G. Lemay, C. Dekker, *Nano Lett.* **2005**, *5*, 137.
[32] D. Krapf, B. M. Quinn, M. Y. Wu, H. W. Zandbergen, C. Dekker, S. G. Lemay, *Nano Lett.* **2006**, *6*, 2531.
[33] J. J. Gooding, A. Chou, J. Q. Liu, D. Losic, J. G. Shapter, D. B. Hibbert, *Electrochem. Commun.* **2007**, *9*, 1677.
[34] I. Heller, A. M. Janssens, J. Mannik, E. D. Minot, S. G. Lemay, C. Dekker, *Nano Lett.* **2008**, *8*, 591.
[35] D. A. Heller, E. S. Jeng, T. K. Yeung, B. M. Martinez, A. E. Moll, J. B. Gastala, M. S. Strano, *Science* **2006**, *311*, 508.
[36] I. Heller, J. Mannik, S. G. Lemay, C. Dekker, *Nano Lett.* **2009**, *9*, 377.
[37] A. Guiseppi-Elie, C. H. Lei, R. H. Baughman, *Nanotechnology* **2002**, *13*, 559.
[38] J. J. Gooding, R. Wibowo, J. Q. Liu, W. R. Yang, D. Losic, S. Orbons, F. J. Mearns, J. G. Shapter, D. B. Hibbert, *J. Am. Chem. Soc.* **2003**, *125*, 9006.
[39] X. Yu, D. Chattopadhyay, I. Galeska, F. Papadimitrakopoulos, J. F. Rusling, *Electrochem. Commun.* **2003**, *5*, 408.
[40] J. Q. Liu, A. Chou, W. Rahmat, M. N. Paddon-Row, J. J. Gooding, *Electroanalysis* **2005**, *17*, 38.
[41] F. Patolsky, Y. Weizmann, I. Willner, *Angew. Chem.* **2004**, *116*, 2165; *Angew. Chem. Int. Ed.* **2004**, *43*, 2113.
[42] J. Li, H. T. Ng, A. Cassell, W. Fan, H. Chen, Q. Ye, J. Koehne, J. Han, M. Meyyappan, *Nano Lett.* **2003**, *3*, 597.
[43] J. Koehne, H. Chen, J. Li, A. M. Cassell, Q. Ye, H. T. Ng, J. Han, M. Meyyappan, *Nanotechnology* **2003**, *14*, 1239.
[44] R. J. Chen, S. Bangsaruntip, K. A. Drouvalakis, N. W. S. Kam, M. Shim, Y. M. Li, W. Kim, P. J. Utz, H. J. Dai, *Proc. Natl. Acad. Sci. USA* **2003**, *100*, 4984.
[45] K. Besteman, J. O. Lee, F. G. M. Wiertz, H. A. Heering, C. Dekker, *Nano Lett.* **2003**, *3*, 727.
[46] B. R. Goldsmith, J. G. Coroneus, V. R. Khalap, A. A. Kane, G. A. Weiss, P. G. Collins, *Science* **2007**, *315*, 77.
[47] D. A. Heller, H. Jin, B. M. Martinez, D. Patel, B. M. Miller, T. K. Yeung, P. V. Jena, C. Hobartner, T. Ha, S. K. Silverman, M. S. Strano, *Nat. Nanotechnol.* **2009**, *4*, 114.
[48] M. C. Hersam, *Nat. Nanotechnol.* **2008**, *3*, 387.
[49] G. G. Wildgoose, C. E. Banks, H. C. Leventis, R. G. Compton, *Microchim. Acta* **2006**, *152*, 187.
[50] J. J. Gooding, *Electrochim. Acta* **2005**, *50*, 3049.
[51] H. J. Dai, *Acc. Chem. Res.* **2002**, *35*, 1035.
[52] L. M. Dai, *Aust. J. Chem.* **2007**, *60*, 472.
[53] T. W. Odom, J. L. Huang, P. Kim, C. M. Lieber, *Nature* **1998**, *391*, 62.
[54] T. W. Odom, J. L. Huang, P. Kim, C. M. Lieber, *J. Phys. Chem. B* **2000**, *104*, 2794.
[55] J. C. Charlier, *Acc. Chem. Res.* **2002**, *35*, 1063.
[56] C. E. Banks, A. Crossley, C. Salter, S. J. Wilkins, R. G. Compton, *Angew. Chem.* **2006**, *118*, 2595; *Angew. Chem. Int. Ed.* **2006**, *45*, 2533.
[57] R. L. McCreery, *Chem. Rev.* **2008**, *108*, 2646.
[58] M. Pumera, *Langmuir* **2007**, *23*, 6453.
[59] X. Dai, G. G. Wildgoose, R. G. Compton, *Analyst* **2006**, *131*, 901.
[60] C. E. Banks, T. J. Davies, G. G. Wildgoose, R. G. Compton, *Chem. Commun.* **2005**, 829.
[61] C. P. Jones, K. Jurkschat, A. Crossley, R. G. Compton, B. L. Riehl, C. E. Banks, *Langmuir* **2007**, *23*, 9501.
[62] A. Chou, T. Böcking, N. K. Singh, J. J. Gooding, *Chem. Commun.* **2005**, 842.
[63] C. E. Banks, X. B. Ji, A. Crossley, R. G. Compton, *Electroanalysis* **2006**, *18*, 2137.
[64] M. Pumera, *Nanoscale Res. Lett.* **2007**, *2*, 87.
[65] X. B. Ji, C. E. Banks, A. Crossley, R. G. Compton, *ChemPhysChem* **2006**, *7*, 1337.
[66] M. Pumera, T. Sasaki, H. Iwai, *Chem. Asian J.* **2008**, *3*, 2046.
[67] K. P. Gong, S. Chakrabarti, L. M. Dai, *Angew. Chem.* **2008**, *120*, 5526; *Angew. Chem. Int. Ed.* **2008**, *47*, 5446.
[68] R. R. Moore, C. E. Banks, R. G. Compton, *Anal. Chem.* **2004**, *76*, 2677.
[69] M. Pumera, *Chem. Eur. J.* **2009**, *15*, 4970.
[70] S. M. Huang, Q. R. Cai, J. Y. Chen, Y. Qian, L. J. Zhang, *J. Am. Chem. Soc.* **2009**, *131*, 2094.
[71] B. L. Liu, W. C. Ren, L. B. Gao, S. S. Li, S. F. Pei, C. Liu, C. B. Jiang, H. M. Cheng, *J. Am. Chem. Soc.* **2009**, *131*, 2082.
[72] S. Niyogi, M. A. Hamon, H. Hu, B. Zhao, P. Bhowmik, R. Sen, M. E. Itkis, R. C. Haddon, *Acc. Chem. Res.* **2002**, *35*, 1105.
[73] A. A. Green, M. C. Hersam, *Nat. Nanotechnol.* **2009**, *4*, 64.
[74] M. J. O'Connell, S. M. Bachilo, C. B. Huffman, V. C. Moore, M. S. Strano, E. H. Haroz, K. L. Rialon, P. J. Boul, W. H. Noon, C. Kittrell, J. P. Ma, R. H. Hauge, R. B. Weisman, R. E. Smalley, *Science* **2002**, *297*, 593.
[75] R. B. Weisman, S. M. Bachilo, *Nano Lett.* **2003**, *3*, 1235.
[76] M. Y. Sfeir, F. Wang, L. M. Huang, C. C. Chuang, J. Hone, S. P. O'Brien, T. F. Heinz, L. E. Brus, *Science* **2004**, *306*, 1540.
[77] D. A. Tsyboulski, S. M. Bachilo, R. B. Weisman, *Nano Lett.* **2005**, *5*, 975.
[78] J. C. Meyer, M. Paillet, T. Michel, A. Moreac, A. Neumann, G. S. Duesberg, S. Roth, J. L. Sauvajol, *Phys. Rev. Lett.* **2005**, *95*, 217401.
[79] S. Berciaud, L. Cognet, P. Poulin, R. B. Weisman, B. Lounis, *Nano Lett.* **2007**, *7*, 1203.
[80] L. Cognet, D. A. Tsyboulski, J. D. R. Rocha, C. D. Doyle, J. M. Tour, R. B. Weisman, *Science* **2007**, *316*, 1465.
[81] H. Jin, D. A. Heller, J. H. Kim, M. S. Strano, *Nano Lett.* **2008**, *8*, 4299.
[82] A. H. Castro Neto, F. Guinea, N. M. R. Peres, K. S. Novoselov, A. K. Geim, *Rev. Mod. Phys.* **2009**, *81*, 109.
[83] K. S. Novoselov, A. K. Geim, S. V. Morozov, D. Jiang, Y. Zhang, S. V. Dubonos, I. V. Grigorieva, A. A. Firsov, *Science* **2004**, *306*, 666.
[84] A. Gupta, G. Chen, P. Joshi, S. Tadigadapa, P. C. Eklund, *Nano Lett.* **2006**, *6*, 2667.

[85] Z. H. Ni, H. M. Wang, J. Kasim, H. M. Fan, T. Yu, Y. H. Wu, Y. P. Feng, Z. X. Shen, *Nano Lett.* **2007**, *7*, 2758.
[86] H. Hibino, H. Kageshima, F. Maeda, M. Nagase, Y. Kobayashi, H. Yamaguchi, *Phys. Rev. B* **2008**, *77*, 075413.
[87] A. K. Geim, K. S. Novoselov, *Nat. Mater.* **2007**, *6*, 183.
[88] J. W. Jiang, H. Tang, B. S. Wang, Z. B. Su, *Phys. Rev. B* **2008**, *77*, 235421.
[89] K. S. Novoselov, D. Jiang, F. Schedin, T. J. Booth, V. V. Khotkevich, S. V. Morozov, A. K. Geim, *Proc. Natl. Acad. Sci. USA* **2005**, *102*, 10451.
[90] J. C. Meyer, A. K. Geim, M. I. Katsnelson, K. S. Novoselov, T. J. Booth, S. Roth, *Nature* **2007**, *446*, 60.
[91] M. H. Gass, U. Bangert, A. L. Bleloch, P. Wang, R. R. Nair, A. K. Geim, *Nat. Nanotechnol.* **2008**, *3*, 676.
[92] V. Geringer, M. Liebmann, T. Echtermeyer, S. Runte, M. Schmidt, R. Ruckamp, M. C. Lemme, M. Morgenstern, *Phys. Rev. Lett.* **2009**, *102*, 076102.
[93] A. Fasolino, J. H. Los, M. I. Katsnelson, *Nat. Mater.* **2007**, *6*, 858.
[94] N. M. R. Peres, *J. Phys. Condens. Matter* **2009**, *21*, 323201.
[95] L. M. Malard, M. A. Pimenta, G. Dresselhaus, M. S. Dresselhaus, *Phys. Rep.* **2009**, *473*, 51.
[96] A. K. Geim, *Science* **2009**, *324*, 1530.
[97] J. Lu, L. T. Drzal, R. M. Worden, I. Lee, *Chem. Mater.* **2007**, *19*, 6240.
[98] P. K. Ang, W. Chen, A. T. S. Wee, K. P. Loh, *J. Am. Chem. Soc.* **2008**, *130*, 14392.
[99] N. G. Shang, P. Papakonstantinou, M. McMullan, M. Chu, A. Stamboulis, A. Potenza, S. S. Dhesi, H. Marchetto, *Adv. Funct. Mater.* **2008**, *18*, 3506.
[100] S. Alwarappan, A. Erdem, C. Liu, C. Z. Li, *J. Phys. Chem. C* **2009**, *113*, 8853.
[101] F. R. F. Fan, S. Park, Y. W. Zhu, R. S. Ruoff, A. J. Bard, *J. Am. Chem. Soc.* **2009**, *131*, 937.
[102] X. Y. Yang, X. Y. Zhang, Z. F. Liu, Y. F. Ma, Y. Huang, Y. Chen, *J. Phys. Chem. C* **2008**, *112*, 17554.
[103] J. Lu, I. Do, L. T. Drzal, R. M. Worden, I. Lee, *ACS Nano* **2008**, *2*, 1825.
[104] C. S. Shan, H. F. Yang, J. F. Song, D. X. Han, A. Ivaska, L. Niu, *Anal. Chem.* **2009**, *81*, 2378.
[105] Y. Wang, Y. M. Li, L. H. Tang, J. Lu, J. H. Li, *Electrochem. Commun.* **2009**, *11*, 889.
[106] K. S. Novoselov, A. K. Geim, S. V. Morozov, D. Jiang, M. I. Katsnelson, I. V. Grigorieva, S. V. Dubonos, A. A. Firsov, *Nature* **2005**, *438*, 197.
[107] K. I. Bolotin, K. J. Sikes, Z. Jiang, M. Klima, G. Fudenberg, J. Hone, P. Kim, H. L. Stormer, *Solid State Commun.* **2008**, *146*, 351.
[108] E. V. Castro, K. S. Novoselov, S. V. Morozov, N. M. R. Peres, J. Dos Santos, J. Nilsson, F. Guinea, A. K. Geim, A. H. Castro Neto, *Phys. Rev. Lett.* **2007**, *99*, 216802.
[109] M. F. Craciun, S. Russo, M. Yamamoto, J. B. Oostinga, A. F. Morpurgo, S. Tarucha, *Nat. Nanotechnol.* **2009**, *4*, 383.
[110] A. Grüneis, C. Attaccalite, L. Wirtz, H. Shiozawa, R. Saito, T. Pichler, A. Rubio, *Phys. Rev. B* **2008**, *78*, 205425.
[111] B. Partoens, F. M. Peeters, *Phys. Rev. B* **2006**, *74*, 075404.
[112] E. A. Henriksen, Z. Jiang, L. C. Tung, M. E. Schwartz, M. Takita, Y. J. Wang, P. Kim, H. L. Stormer, *Phys. Rev. Lett.* **2008**, *100*, 087403.
[113] R. S. Deacon, K. C. Chuang, R. J. Nicholas, K. S. Novoselov, A. K. Geim, *Phys. Rev. B* **2007**, *76*, 081406.
[114] Z. Jiang, E. A. Henriksen, L. C. Tung, Y. J. Wang, M. E. Schwartz, M. Y. Han, P. Kim, H. L. Stormer, *Phys. Rev. Lett.* **2007**, *98*, 197403.
[115] M. Orlita, C. Faugeras, G. Martinez, D. K. Maude, M. L. Sadowski, J. M. Schneider, M. Potemski, *J. Phys. Condens. Matter* **2008**, *20*, 454223.
[116] M. Orlita, C. Faugeras, J. M. Schneider, G. Martinez, D. K. Maude, M. Potemski, *Phys. Rev. Lett.* **2009**, *102*, 166401.
[117] P. Plochocka, C. Faugeras, M. Orlita, M. L. Sadowski, G. Martinez, M. Potemski, M. O. Goerbig, J. N. Fuchs, C. Berger, W. A. de Heer, *Phys. Rev. Lett.* **2008**, *100*, 087401.
[118] I. A. Luk'yanchuk, Y. Kopelevich, M. El Marssi, *Physica B* **2009**, *404*, 404.
[119] L. M. Malard, J. Nilsson, D. C. Elias, J. C. Brant, F. Plentz, E. S. Alves, A. H. Castro, M. A. Pimenta, *Phys. Rev. B* **2007**, *76*, 201401.
[120] A. C. Ferrari, J. C. Meyer, V. Scardaci, C. Casiraghi, M. Lazzeri, F. Mauri, S. Piscanec, D. Jiang, K. S. Novoselov, S. Roth, A. K. Geim, *Phys. Rev. Lett.* **2006**, *97*, 187401.
[121] D. Graf, F. Molitor, K. Ensslin, C. Stampfer, A. Jungen, C. Hierold, L. Wirtz, *Nano Lett.* **2007**, *7*, 238.
[122] J. Yan, Y. B. Zhang, P. Kim, A. Pinczuk, *Phys. Rev. Lett.* **2007**, *98*, 166802.
[123] R. R. Nair, P. Blake, A. N. Grigorenko, K. S. Novoselov, T. J. Booth, T. Stauber, N. M. R. Peres, A. K. Geim, *Science* **2008**, *320*, 1308.
[124] K. S. Novoselov, E. McCann, S. V. Morozov, V. I. Fal'ko, M. I. Katsnelson, U. Zeitler, D. Jiang, F. Schedin, A. K. Geim, *Nat. Phys.* **2006**, *2*, 177.
[125] J. H. Chen, C. Jang, S. D. Xiao, M. Ishigami, M. S. Fuhrer, *Nat. Nanotechnol.* **2008**, *3*, 206.
[126] H. Hibino, H. Kageshima, M. Kotsugi, F. Maeda, F. Z. Guo, Y. Watanabe, *Phys. Rev. B* **2009**, *79*, 125437.
[127] Z. H. Ni, W. Chen, X. F. Fan, J. L. Kuo, T. Yu, A. T. S. Wee, Z. X. Shen, *Phys. Rev. B* **2008**, *77*, 115416.
[128] H. M. Wang, Y. H. Wu, Z. H. Ni, Z. X. Shen, *Appl. Phys. Lett.* **2008**, *92*, 053504.
[129] L. Brey, J. J. Palacios, *Phys. Rev. B* **2008**, *77*, 041403.
[130] V. C. Tung, M. J. Allen, Y. Yang, R. B. Kaner, *Nat. Nanotechnol.* **2009**, *4*, 25.
[131] Z. S. Wu, W. C. Ren, L. B. Gao, J. P. Zhao, Z. P. Chen, B. L. Liu, D. M. Tang, B. Yu, C. B. Jiang, H. M. Cheng, *ACS Nano* **2009**, *3*, 411.
[132] Z. H. Ni, Y. Y. Wang, T. Yu, Y. M. You, Z. X. Shen, *Phys. Rev. B* **2008**, *77*, 235403.
[133] M. Moreno-Moreno, A. Castellanos-Gomez, G. Rubio-Bollinger, J. Gomez-Herrero, N. Agrait, *Small* **2009**, *5*, 924.
[134] F. Schedin, A. K. Geim, S. V. Morozov, E. W. Hill, P. Blake, M. I. Katsnelson, K. S. Novoselov, *Nat. Mater.* **2007**, *6*, 652.
[135] T. Enoki, Y. Kobayashi, K. Fukui, *Int. Rev. Phys. Chem.* **2007**, *26*, 609.
[136] V. B. Shenoy, C. D. Reddy, A. Ramasubramaniam, Y. W. Zhang, *Phys. Rev. Lett.* **2008**, *101*, 245501.
[137] F. R. F. Fan, A. J. Bard, *Science* **1995**, *267*, 871.
[138] S. M. Nie, S. R. Emery, *Science* **1997**, *275*, 1102.
[139] H. P. Lu, L. Y. Xun, X. S. Xie, *Science* **1998**, *282*, 1877.
[140] E. Katz, I. Willner, *ChemPhysChem* **2004**, *5*, 1085.
[141] I. Dumitrescu, P. R. Unwin, N. R. Wilson, J. V. Macpherson, *Anal. Chem.* **2008**, *80*, 3598.
[142] Z. F. Liu, Z. Y. Shen, T. Zhu, S. F. Hou, L. Z. Ying, Z. J. Shi, Z. N. Gu, *Langmuir* **2000**, *16*, 3569.
[143] A. Chou, P. K. Eggers, M. N. Paddon-Row, J. J. Gooding, *J. Phys. Chem. C* **2009**, *113*, 3203.
[144] L. M. Dai, A. W. H. Mau, *Adv. Mater.* **2001**, *13*, 899.
[145] L. T. Qu, F. Du, L. M. Dai, *Nano Lett.* **2008**, *8*, 2682.
[146] B. Q. Wei, R. Vajtai, Y. Jung, J. Ward, R. Zhang, G. Ramanath, P. M. Ajayan, *Nature* **2002**, *416*, 495.
[147] L. M. Dai, A. Patil, X. Y. Gong, Z. X. Guo, L. Q. Liu, Y. Liu, D. B. Zhu, *ChemPhysChem* **2003**, *4*, 1150.
[148] P. Diao, Z. F. Liu, *J. Phys. Chem. B* **2005**, *109*, 20906.
[149] J. K. Campbell, L. Sun, R. M. Crooks, *J. Am. Chem. Soc.* **1999**, *121*, 3779.

[150] I. Heller, J. Kong, K. A. Williams, C. Dekker, S. G. Lemay, *J. Am. Chem. Soc.* **2006**, *128*, 7353.
[151] J. Wang, M. Musameh, Y. H. Lin, *J. Am. Chem. Soc.* **2003**, *125*, 2408.
[152] M. Musameh, J. Wang, A. Merkoci, Y. H. Lin, *Electrochem. Commun.* **2002**, *4*, 743.
[153] Q. Wang, H. Tang, Q. J. Me, L. Tan, Y. Y. Zhang, B. Li, S. Z. Yao, *Electrochim. Acta* **2007**, *52*, 6630.
[154] R. T. Kachoosangi, M. M. Musameh, I. Abu-Yousef, J. M. Yousef, S. M. Kanan, L. Xiao, S. G. Davies, A. Russell, R. G. Compton, *Anal. Chem.* **2009**, *81*, 435.
[155] X. Yu, B. Munge, V. Patel, G. Jensen, A. Bhirde, J. D. Gong, S. N. Kim, J. Gillespie, J. S. Gutkind, F. Papadimitrakopoulos, J. F. Rusling, *J. Am. Chem. Soc.* **2006**, *128*, 11199.
[156] M. Gao, L. M. Dai, G. G. Wallace, *Electroanalysis* **2003**, *15*, 1089.
[157] L. T. Qu, L. M. Dai, *J. Am. Chem. Soc.* **2005**, *127*, 10806.
[158] L. T. Qu, L. M. Dai, E. Osawa, *J. Am. Chem. Soc.* **2006**, *128*, 5523.
[159] J. C. Claussen, A. D. Franklin, A. ul Haque, D. M. Porterfield, T. S. Fisher, *ACS Nano* **2009**, *3*, 37.
[160] H. Hu, Y. C. Ni, V. Montana, R. C. Haddon, V. Parpura, *Nano Lett.* **2004**, *4*, 507.
[161] G. G. Wallace, S. E. Moulton, G. M. Clark, *Science* **2009**, *324*, 185.
[162] E. W. Keefer, B. R. Botterman, M. I. Romero, A. F. Rossi, G. W. Gross, *Nat. Nanotechnol.* **2008**, *3*, 434.
[163] N. W. S. Kam, E. Jan, N. A. Kotov, *Nano Lett.* **2009**, *9*, 273.
[164] Y. Q. Lin, N. N. Zhu, P. Yu, L. Su, L. Q. Mao, *Anal. Chem.* **2009**, *81*, 2067.
[165] S. K. Smart, A. I. Cassady, G. Q. Lu, D. J. Martin, *Carbon* **2006**, *44*, 1034.
[166] V. E. Kagan, H. Bayir, A. A. Shvedova, *Nanomedicine* **2005**, *1*, 313.
[167] M. J. Moghaddam, S. Taylor, M. Gao, S. M. Huang, L. M. Dai, M. J. McCall, *Nano Lett.* **2004**, *4*, 89.
[168] W. R. Yang, M. Moghaddam, S. Taylor, B. Bojarski, L. Wieczorek, J. Herrmann, M. McCall, *Chem. Phys. Lett.* **2007**, *443*, 169.
[169] P. G. He, L. M. Dai, *Chem. Commun.* **2004**, 348.
[170] P. G. He, S. N. Li, L. M. Dai, *Synth. Met.* **2005**, *154*, 17.
[171] S. M. Shamah, J. M. Healy, S. T. Cload, *Acc. Chem. Res.* **2008**, *41*, 130.
[172] G. A. Zelada, J. Riu, A. Düzgün, F. X. Rius, *Angew. Chem.* **2009**, *121*, 7470; *Angew. Chem. Int. Ed.* **2009**, *48*, 7334.
[173] F. Patolsky, B. P. Timko, G. F. Zheng, C. M. Lieber, *MRS Bull.* **2007**, *32*, 142.
[174] G. F. Zheng, F. Patolsky, Y. Cui, W. U. Wang, C. M. Lieber, *Nat. Biotechnol.* **2005**, *23*, 1294.
[175] F. Patolsky, G. F. Zheng, O. Hayden, M. Lakadamyali, X. W. Zhuang, C. M. Lieber, *Proc. Natl. Acad. Sci. USA* **2004**, *101*, 14017.
[176] P. G. Collins, A. Zettl, H. Bando, A. Thess, R. E. Smalley, *Science* **1997**, *278*, 100.
[177] P. G. Collins, K. Bradley, M. Ishigami, A. Zettl, *Science* **2000**, *287*, 1801.
[178] A. Star, J. C. P. Gabriel, K. Bradley, G. Gruner, *Nano Lett.* **2003**, *3*, 459.
[179] S. Boussaad, N. J. Tao, R. Zhang, T. Hopson, L. A. Nagahara, *Chem. Commun.* **2003**, 1502.
[180] A. Star, E. Tu, J. Niemann, J. C. P. Gabriel, C. S. Joiner, C. Valcke, *Proc. Natl. Acad. Sci. USA* **2006**, *103*, 921.
[181] K. Maehashi, T. Katsura, K. Kerman, Y. Takamura, K. Matsumoto, E. Tamiya, *Anal. Chem.* **2007**, *79*, 782.
[182] C. C. Cid, J. Riu, A. Maroto, F. X. Rius, *Analyst* **2008**, *133*, 1001.
[183] E. L. Gui, L. J. Li, K. K. Zhang, Y. P. Xu, X. C. Dong, X. N. Ho, P. S. Lee, J. Kasim, Z. X. Shen, J. A. Rogers, S. G. Mhaisalkar, *J. Am. Chem. Soc.* **2007**, *129*, 14427.
[184] K. Bradley, J. C. P. Gabriel, M. Briman, A. Star, G. Gruner, *Phys. Rev. Lett.* **2003**, *91*, 218301.
[185] M. T. Martinez, Y. C. Tseng, N. Ormategui, I. Loinaz, R. Eritja, J. Bokor, *Nano Lett.* **2009**, *9*, 530.
[186] P. J. Choi, L. Cai, K. Frieda, S. Xie, *Science* **2008**, *322*, 442.
[187] H. G. Sudibya, J. M. Ma, X. C. Dong, S. Ng, L. J. Li, X. W. Liu, P. Chen, *Angew. Chem.* **2009**, *121*, 2761; *Angew. Chem. Int. Ed.* **2009**, *48*, 2723.
[188] R. A. Villamizar, A. Maroto, F. X. Rius, I. Inza, M. J. Figueras, *Biosens. Bioelectron.* **2008**, *24*, 279.
[189] H. M. So, D. W. Park, E. K. Jeon, Y. H. Kim, B. S. Kim, C. K. Lee, S. Y. Choi, S. C. Kim, H. Chang, J. O. Lee, *Small* **2008**, *4*, 197.
[190] C. W. Wang, C. Y. Pan, H. C. Wu, P. Y. Shih, C. C. Tsai, K. T. Liao, L. L. Lu, W. H. Hsieh, C. D. Chen, Y. T. Chen, *Small* **2007**, *3*, 1350.
[191] X. J. Zhou, J. M. Moran-Mirabal, H. G. Craighead, P. L. McEuen, *Nat. Nanotechnol.* **2007**, *2*, 185.
[192] D. X. Cui, B. F. Pan, H. Zhang, F. Gao, R. Wu, J. P. Wang, R. He, T. Asahi, *Anal. Chem.* **2008**, *80*, 7996.
[193] M. Engel, J. P. Small, M. Steiner, M. Freitag, A. A. Green, M. C. Hersam, P. Avouris, *ACS Nano* **2008**, *2*, 2445.
[194] P. Avouris, M. Freitag, V. Perebeinos, *Nat. Photonics* **2008**, *2*, 341.
[195] P. Avouris, M. Freitag, V. Perebeinos, *Carbon Nanotubes* **2008**, *111*, 423.
[196] R. H. Yang, Z. W. Tang, J. L. Yan, H. Z. Kang, Y. M. Kim, Z. Zhu, W. H. Tan, *Anal. Chem.* **2008**, *80*, 7408.
[197] B. C. Satishkumar, L. O. Brown, Y. Gao, C. C. Wang, H. L. Wang, S. K. Doorn, *Nat. Nanotechnol.* **2007**, *2*, 560.
[198] X. Y. Gao, G. M. Xing, Y. L. Yang, X. L. Shi, R. Liu, W. G. Chu, L. Jing, F. Zhao, C. Ye, H. Yuan, X. H. Fang, C. Wang, Y. L. Zhao, *J. Am. Chem. Soc.* **2008**, *130*, 9190.
[199] E. S. Jeng, P. W. Barone, J. D. Nelson, M. S. Strano, *Small* **2007**, *3*, 1602.
[200] E. S. Jeng, A. E. Moll, A. C. Roy, J. B. Gastala, M. S. Strano, *Nano Lett.* **2006**, *6*, 371.
[201] D. Li, R. B. Kaner, *Science* **2008**, *320*, 1170.
[202] S. Park, R. S. Ruoff, *Nat. Nanotechnol.* **2009**, *4*, 217.
[203] C. Gomez-Navarro, R. T. Weitz, A. M. Bittner, M. Scolari, A. Mews, M. Burghard, K. Kern, *Nano Lett.* **2007**, *7*, 3499.
[204] Z. Q. Wei, D. E. Barlow, P. E. Sheehan, *Nano Lett.* **2008**, *8*, 3141.
[205] D. Yang, A. Velamakanni, G. Bozoklu, S. Park, M. Stoller, R. D. Piner, S. Stankovich, I. Jung, D. A. Field, C. A. Ventrice, R. S. Ruoff, *Carbon* **2009**, *47*, 145.
[206] Y. Hernandez, V. Nicolosi, M. Lotya, F. M. Blighe, Z. Y. Sun, S. De, I. T. McGovern, B. Holland, M. Byrne, Y. K. Gun'ko, J. J. Boland, P. Niraj, G. Duesberg, S. Krishnamurthy, R. Goodhue, J. Hutchison, V. Scardaci, A. C. Ferrari, J. N. Coleman, *Nat. Nanotechnol.* **2008**, *3*, 563.
[207] X. L. Li, G. Y. Zhang, X. D. Bai, X. M. Sun, X. R. Wang, E. Wang, H. J. Dai, *Nat. Nanotechnol.* **2008**, *3*, 538.
[208] K. S. Kim, Y. Zhao, H. Jang, S. Y. Lee, J. M. Kim, J. H. Ahn, P. Kim, J. Y. Choi, B. H. Hong, *Nature* **2009**, *457*, 706.
[209] W. A. de Heer, C. Berger, X. S. Wu, P. N. First, E. H. Conrad, X. B. Li, T. B. Li, M. Sprinkle, J. Hass, M. L. Sadowski, M. Potemski, G. Martinez, *Solid State Commun.* **2007**, *143*, 92.
[210] T. Seyller, A. Bostwick, K. V. Emtsev, K. Horn, L. Ley, J. L. McChesney, T. Ohta, J. D. Riley, E. Rotenberg, F. Speck, *Phys. Status Solidi B* **2008**, *245*, 1436.
[211] Q. H. Wang, M. C. Hersam, *Nat. Chem.* **2009**, *1*, 206.

[212] C. Berger, Z. M. Song, T. B. Li, X. B. Li, A. Y. Ogbazghi, R. Feng, Z. T. Dai, A. N. Marchenkov, E. H. Conrad, P. N. First, W. A. de Heer, *J. Phys. Chem. B* **2004**, *108*, 19912.
[213] A. Reina, X. T. Jia, J. Ho, D. Nezich, H. B. Son, V. Bulovic, M. S. Dresselhaus, J. Kong, *Nano Lett.* **2009**, *9*, 30.
[214] X. S. Li, W. W. Cai, J. H. An, S. Kim, J. Nah, D. X. Yang, R. Piner, A. Velamakanni, I. Jung, E. Tutuc, S. K. Banerjee, L. Colombo, R. S. Ruoff, *Science* **2009**, *324*, 1312.
[215] S. Muller, K. Müllen, *Philos. Trans. R. Soc. London Ser. A* **2007**, *365*, 1453.
[216] J. Wu, W. Pisula, K. Müllen, *Chem. Rev.* **2007**, *107*, 718.
[217] L. J. Zhi, K. Müllen, *J. Mater. Chem.* **2008**, *18*, 1472.
[218] X. Wang, L. J. Zhi, N. Tsao, Z. Tomovic, J. L. Li, K. Müllen, *Angew. Chem.* **2008**, *120*, 3032; *Angew. Chem. Int. Ed.* **2008**, *47*, 2990.
[219] M. Choucair, P. Thordarson, J. A. Stride, *Nat. Nanotechnol.* **2009**, *4*, 30.
[220] M. Qazi, T. Vogt, G. Koley, *Appl. Phys. Lett.* **2007**, *91*, 233101.
[221] J. T. Robinson, F. K. Perkins, E. S. Snow, Z. Q. Wei, P. E. Sheehan, *Nano Lett.* **2008**, *8*, 3137.
[222] R. Arsat, M. Breedon, M. Shafiei, P. G. Spizziri, S. Gilje, R. B. Kaner, K. Kalantar-Zadeh, W. Wlodarski, *Chem. Phys. Lett.* **2009**, *467*, 344.
[223] J. D. Fowler, M. J. Allen, V. C. Tung, Y. Yang, R. B. Kaner, B. H. Weiller, *ACS Nano* **2009**, *3*, 301.
[224] G. H. Lu, L. E. Ocola, J. H. Chen, *Appl. Phys. Lett.* **2009**, *94*, 083111.
[225] Y. P. Dan, Y. Lu, N. J. Kybert, Z. T. Luo, A. T. C. Johnson, *Nano Lett.* **2009**, *9*, 1472.
[226] O. Leenaerts, B. Partoens, F. M. Peeters, *Phys. Rev. B* **2008**, *77*, 125416.
[227] Z. M. Ao, J. Yang, S. Li, Q. Jiang, *Chem. Phys. Lett.* **2008**, *461*, 276.
[228] Y. H. Zhang, Y. B. Chen, K. G. Zhou, C. H. Liu, J. Zeng, H. L. Zhang, Y. Peng, *Nanotechnology* **2009**, *20*.
[229] Y. Ohno, K. Maehashi, U. Yamashiro, K. Matsumoto, *Nano Lett.* **2009**, *9*, 3318.
[230] N. Mohanty, V. Berry, *Nano Lett.* **2008**, *8*, 4469.
[231] C. H. Lu, H. H. Yang, C. L. Zhu, X. Chen, G. N. Chen, *Angew. Chem.* **2009**, *121*, 4879; *Angew. Chem. Int. Ed.* **2009**, *48*, 4785.
[232] A. Salimi, R. G. Compton, R. Hallaj, *Anal. Biochem.* **2004**, *333*, 49.
[233] B. M. Quinn, C. Dekker, S. G. Lemay, *J. Am. Chem. Soc.* **2005**, *127*, 6146.
[234] K. B. Wu, J. J. Fei, S. S. Hu, *Anal. Biochem.* **2003**, *318*, 100.
[235] M. N. Zhang, K. P. Gong, H. W. Zhang, L. Q. Mao, *Biosens. Bioelectron.* **2005**, *20*, 1270.
[236] N. Varghese, U. Mogera, A. Govindaraj, A. Das, P. K. Maiti, A. K. Sood, C. N. R. Rao, *ChemPhysChem* **2009**, *10*, 206.
[237] G. A. Crespo, S. Macho, J. Bobacka, F. X. Rius, *Anal. Chem.* **2009**, *81*, 676.
[238] G. A. Crespo, S. Macho, F. X. Rius, *Anal. Chem.* **2008**, *80*, 1316.
[239] Z. K. Tang, L. Y. Zhang, N. Wang, X. X. Zhang, G. H. Wen, G. D. Li, J. N. Wang, C. T. Chan, P. Sheng, *Science* **2001**, *292*, 2462.
[240] L. Song, L. Ci, W. Gao, P. M. Ajayan, *ACS Nano* **2009**, *3*, 1353.
[241] Y. M. Lin, P. Avouris, *Nano Lett.* **2008**, *8*, 2119.
[242] Q. H. Shao, G. X. Liu, D. Teweldebrhan, A. A. Balandin, S. Runryantsev, M. S. Shur, D. Yan, *IEEE Electron Device Lett.* **2009**, *30*, 288.
[243] P. C. Collins, M. S. Arnold, P. Avouris, *Science* **2001**, *292*, 706.
[244] R. Krupke, F. Hennrich, H. von Lohneysen, M. M. Kappes, *Science* **2003**, *301*, 344.
[245] M. Zheng, A. Jagota, M. S. Strano, A. P. Santos, P. Barone, S. G. Chou, B. A. Diner, M. S. Dresselhaus, R. S. McLean, G. B. Onoa, G. G. Samsonidze, E. D. Semke, M. Usrey, D. J. Walls, *Science* **2003**, *302*, 1545.
[246] M. S. Strano, C. A. Dyke, M. L. Usrey, P. W. Barone, M. J. Allen, H. W. Shan, C. Kittrell, R. H. Hauge, J. M. Tour, R. E. Smalley, *Science* **2003**, *301*, 1519.
[247] M. Kanungo, H. Lu, G. G. Malliaras, G. B. Blanchet, *Science* **2009**, *323*, 234.
[248] M. Ishigami, J. H. Chen, W. G. Cullen, M. S. Fuhrer, E. D. Williams, *Nano Lett.* **2007**, *7*, 1643.
[249] U. Stoberl, U. Wurstbauer, W. Wegscheider, D. Weiss, J. Eroms, *Appl. Phys. Lett.* **2008**, *93*, 051906.
[250] Y. H. Chen, Z. Iqbal, S. Mitra, *Adv. Funct. Mater.* **2007**, *17*, 3946.
[251] A. Nish, J. Y. Hwang, J. Doig, R. J. Nicholas, *Nat. Nanotechnol.* **2007**, *2*, 640.
[252] M. K. Gheith, T. C. Pappas, A. V. Liopo, V. A. Sinani, B. S. Shim, M. Motamedi, J. R. Wicksted, N. A. Kotov, *Adv. Mater.* **2006**, *18*, 2975.
[253] T. R. Fadel, E. R. Steenblock, E. Stern, N. Li, X. Wang, G. L. Haller, L. D. Pfefferle, T. M. Fahmy, *Nano Lett.* **2008**, *8*, 2070.
[254] P. Chakravarty, R. Marches, N. S. Zimmerman, A. D. E. Swafford, P. Bajaj, I. H. Musselman, P. Pantano, R. K. Draper, E. S. Vitetta, *Proc. Natl. Acad. Sci. USA* **2008**, *105*, 8697.
[255] X. Chen, A. Kis, A. Zettl, C. R. Bertozzi, *Proc. Natl. Acad. Sci. USA* **2007**, *104*, 8218.

